J|A|C|S
ARTICLES

Oxygen Atom Transfer Reactions from Isolated (Oxo)manganese(V) Corroles to Sulfides

Anil Kumar,[†] Israel Goldberg,*[‡] Mark Botoshansky,[†] Yekaterina Buchman,[†] and Zeev Gross*[†]

Schulich Faculty of Chemistry, Technion-Israel Institute of Technology, Haifa 32000, Israel, and School of Chemistry, Tel-Aviv University, Tel-Aviv 69978, Israel

Received June 20, 2010; E-mail: chr10zg@tx.technion.ac.il; goldberg@post.tau.ac.il

Abstract: A series of five free-base corroles were metalated and brominated to form 10 manganese(III) corroles. Two of the free-base corroles and six manganese(III) corroles were analyzed by X-ray crystallography, including one complex that may be considered a transition-state analogue of oxygen atom transfer (OAT) from (oxo)manganese(V) to thioanisole. Oxidation by ozone allowed for *isolation* of the 10 corresponding (oxo)manganese(V) corroles, whose characterization by ^{1}H and ^{19}F NMR spectroscopy and electrochemistry revealed a low-spin and triply bound manganese−oxygen moiety. Mechanistic insight was obtained by investigating their reactivity regarding *stoichiometric* OAT to a series of *p*-thioanisoles, revealing a magnitude difference on the order of 5 between the *β*-pyrrole brominated (oxo)manganese(V) corroles relative to the nonbrominated analogues. The main conclusion is that the (oxo)manganese(V) corroles are legitimate OAT agents under conditions where proposed oxidant-coordinated reaction intermediates are irrelevant. Large negative Hammett *ρ* constants are obtained for the more reactive (oxo)manganese(V) corroles, consistent with expectation for such electrophilic species. The least reactive complexes display very little selectivity to the electron-richness of the sulfides, as well as a non-first-order dependence on the concentration of (oxo)manganese(V) corrole. This suggests that disproportionation of the original (oxo)manganese(V) corrole to (oxo)manganese(IV) and (oxo)manganese(VI) corroles, followed by substrate oxidation by the latter complex, gains importance when the direct OAT process becomes progressively less favorable.

1. Introduction

High-valent metal−oxo species are key intermediates in catalytic oxygen atom transfer (OAT) to hydrogen abstraction reactions from organic and inorganic substrates.[1] Extensive literature is available on 20-membered ring macrocyclic porphyrin−metal complexes, which mimic many functions of heme-containing enzymes.[2] Manganese(III) porphyrins are versatile catalysts for oxygen transfer reactions, but the corresponding (oxo)manganese(V) complexes have been adequately characterized much later than initially proposed.[3−6] Research on metal complexes of corroles, the unsaturated analogues of the corrin ligand present in the cobalt-containing vitamin B_{12} enzyme, were much less studied for decades,[7] a situation that changed very much after the discovery of facile synthesis of

meso-substituted free-base corroles in 1999.[8,9] One intriguing finding is that corrole-chelated metal−oxo and metal−nitrido complexes are much more stable than in other coordination environments. Nevertheless, manganese(III) corroles are still

† Technion-Israel Institute of Technology.
‡ Tel-Aviv University.
(1) (a) Que, L., Jr. In *Bioinorganic Catalysis*; Reedijk, J., Ed.; Marcell Dekker, Inc.: New York, 1993; pp 347−393. (b) *Biomimetic Oxidations Catalyzed by Transition Metal Complexes*; Meunier, B. , Ed.; Imperial College Press: London, 2000. (c) Sheldon, R. A., Ed. *Metalloporphyrins in Catalytic Oxidations*; Marcel Dekker: New York, 1994.
(2) (a) Collman, J. P.; Zhang, X.; Lee, V. J.; Uffelman, E. S.; Brauman, J. I. *Science* **1993**, *261*, 1404−1411. (c) Groves, J. T.; Shalyaev, K.; Lee, J. *Porphyrin Handbook* **2000**, *4*, 17−40. (d) Groves, J. T. In *Cytochrome-P450: Structure, Mechanism, and Biochemistry*, 3rd ed.; Ortiz de Montellano, P. R., Ed; Kluwer Academic/Plenum Publisher: New York, 2005; pp 1−43. (e) Nam, W. *Acc. Chem. Res.* **2007**, *48*, 6582−6585.

(3) (a) Groves, J. T.; Nemo, T. E.; Myers, R. S. *J. Am. Chem. Soc.* **1979**, *101*, 1032−1033. (b) Hill, C. L.; Schardt, B. C. *J. Am. Chem. Soc.* **1980**, *102*, 6374−6375. (c) Groves, J. T.; Kruper, W. J.; Haushalter, R. C. *J. Am. Chem. Soc.* **1980**, *102*, 6375−6377. (d) Groves, J. T.; Haushalter, R. C.; Nakamura, M.; Nemo, T. E.; Evans, B. J. *J. Am. Chem. Soc.* **1981**, *103*, 2884−2886. (e) Trautwein, A. X.; Bill, E.; Bominaar, E. L.; Winkler, H. *Struct. Bonding (Berlin)* **1991**, *78*, 83−95. (f) Jin, N.; Groves, J. T. *J. Am. Chem. Soc.* **1999**, *121*, 2923−2924. (g) Jin, N.; Bourassa, J. L.; Tizio, S. C.; Groves, J. T. *Angew. Chem., Int. Ed.* **2000**, *39*, 3849−3851. (h) Groves, J. T. *J. Inorg. Biochem.* **2006**, *100*, 434−447. (i) Song, W. J.; Seo, M. S.; George, S. D.; Ohta, T.; Song, R.; Kang, M. J.; Tosha, T.; Kitagawa, T.; Solomon, E. I. *J. Am. Chem. Soc.* **2007**, *129*, 1268−1277. (j) Gross, Z. *Angew. Chem., Int. Ed.* **2008**, *47*, 2737−2739.
(4) Nam, W.; Kim, I.; Lim, M. H.; Choi, H. J.; Lee, S. J.; Jang, H. G. *Chem.—Eur. J.* **2002**, *8*, 2067−2071.
(5) (a) Zhang, R.; Newcomb, M. *J. Am. Chem. Soc.* **2003**, *125*, 12418−12419. (b) Zhang, R.; Horner, J. H.; Newcomb, M. *J. Am. Chem. Soc.* **2005**, *127*, 6573−6582.
(6) Shimazaki, Y.; Nagano, T.; Takesue, H.; Ye, B.-H.; Tani, F.; Naruta, Y. *Angew. Chem., Int. Ed.* **2004**, *43*, 98−100.
(7) (a) Paolesse, R. In *The Porphyrin Handbook*; Kadish, K. M., Smith, K. M., Guilard, R., Eds.; Academic Press: New York, 2000; Vol. 2, Chapter 11. (b) Erben, C.; Will, S.; Kadish, K. M. In *The Porphyrin Handbook*; Kadish, K. M., Smith, K. M., Guilard, R., Eds.; Academic Press: New York, 2000; Vol. 2, Chapter 12. . (c) Sessler, J. L.; Weghorn, S. J. *Expanded, Contacted, and Isomeric Porphyrins*; Pergamon: Oxford, 1997.

Scheme 1. Proposed Reaction Mechanisms for Oxidation Reactions Catalyzed by Manganese(III) Complexes of Corroles and Corrolazine (cor = the trianonic form of corrole or corrolazine)
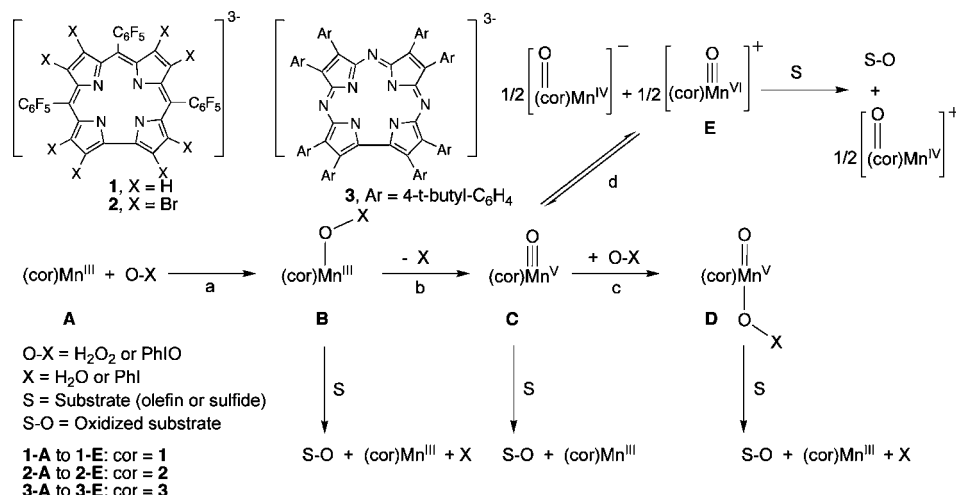
good catalysts for OAT reactions from different oxidants to organic substrates such as olefins and sulfides.[10,11] The corresponding reaction mechanism remains puzzling, because the isolation and spectroscopic characterization of an authentic (oxo)manganese(V) corrole revealed that it is inert toward OAT to olefins.[11b,i] A similar situation exists for corrolazine (tetrazacorroles) whose (oxo)manganese(V) complexes are even more stable.[11f]

The earliest provided explanation for the above paradox was that the active oxidant is not (oxo)manganese(V) corrole (**C** in Scheme 1), but an (oxo)manganese(VI) derivative formed via disproportionation of the former (pathway d and complex **E**, Scheme 1).[11b] Two other mechanistic proposals originated from investigations by the groups of Collman[12] and Goldberg[13] for OAT reactions from (oxo)manganese(V) complexes of corroles and corrolazine, respectively. The former pointed toward the importance of oxidant-coordinated manganese(III) (**B** in Scheme 1) and the latter to Lewis-acid like activation of the oxidant by (oxo)manganese(V) (**D** in Scheme 1), with iodosylbenzene as the oxidant in both cases. Newcomb and co-workers used laser flash photolysis methods to create (oxo)manganese(V) corroles via a different route and investigated their reactivity toward organic substrates.[14] Their results were explained by one of the two following mechanisms: oxidation by (oxo)manganese(VI), produced at low concentration via disproportion
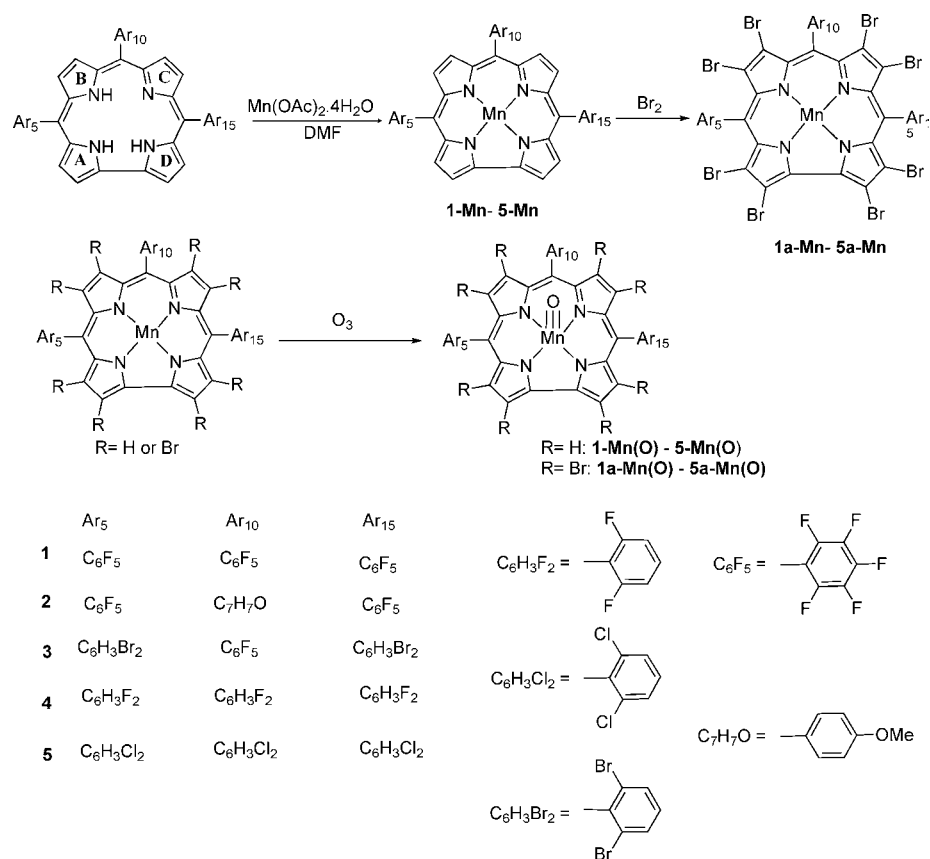
of (oxo)manganese(V), or oxidation by free (oxo)manganese(V) that equilibrates with inactive sequestered forms. The most illuminating results described in their study was that an increase in the electron withdrawing effects of the corrole ligand provided (oxo)manganese(V) species that were less reactive. Both models are consistent with this finding because the populations of active oxidants may be expected to be smaller for the electron-poor complexes. It also provides a rationalization for the stability of the high-electron demand corrolazine (oxo)manganese(V) species observed by Goldberg and co-workers. Newcomb's conclusion was that, while multiple oxidant forms might be involved under catalytic turnover conditions, a single oxidant form appears to be involved when the (oxo)metal species are formed photochemically. Interestingly, similar mechanistic puzzles do exist for (nitrido)manganese(V) and (amido)manganese(V) corroles;[11i,15] cases of increased electron demand have been reported for metalloporphyrins as well.[16]

The above introduction suggests that valuable information may be acquired from studies of OAT reactions from *isolated* (oxo)manganese(V) corroles to organic substrates, not at least because species such as B and D of Scheme 1 are certainly not

(8) For the original breakthroughs, see: (a) Gross, Z.; Galili, N.; Saltsman, I. *Angew. Chem., Int. Ed.* **1999**, *38*, 1427–1429. (b) Gross, Z.; Galili, N.; Simkhovich, L.; Saltsman, I.; Botoshansky, M.; Bläser, D.; Boese, R.; Goldberg, I. *Org. Lett.* **1999**, *1*, 599–602. (c) Gross, Z.; Simkhovich, L.; Galili, N. *Chem. Commun.* **1999**, 599–600. (d) Gross, Z.; Galili, N. *Angew. Chem., Int. Ed.* **1999**, *38*, 2366–2369. (e) Paolesse, R.; Jaquinod, L.; Nurco, D. J.; Mini, S.; Sagone, F.; Boschi, T.; Smith, K. M. *Chem. Commun.* **1999**, 1307–1308.

(9) For recent reviews, see: (a) Gryko, D. T. *Eur. J. Org. Chem.* **2002**, 1735–1743. (b) Ghosh, A. *Angew. Chem., Int. Ed.* **2004**, *43*, 1918. (c) Gryko, D. T.; Koszarna, B. *Synthesis* **2004**, *13*, 2205–2209. (d) Koszarna, B.; Gryko, D. T. *J. Org. Chem.* **2006**, *71*, 3707–3717. (e) Broring, M.; Funk, M.; Milsmann, C. *J. Porphyrins Phthalocyanines* **2009**, *13*, 107–113.

(10) (a) Simkhovich, L.; Mahammed, A.; Goldberg, I.; Gross, Z. *Chem.—Eur. J.* **2001**, *7*, 1041. (b) Simkhovich, L.; Gross, Z. *Tetrahedron Lett.* **2001**, *42*, 8089. (c) Mahammed, A.; Gross, Z. *Angew. Chem., Int. Ed.* **2006**, *45*, 6544–6547. (d) Aviv, I.; Gross, Z. *Chem. Commun.* **2007**, 1987–1999. (e) Aviv-Harel, I.; Gross, Z. *Chem.—Eur. J.* **2009**, *15*, 8382–8384. (f) Goldberg, D. P. *Acc. Chem. Res.* **2007**, *40*, 626–634. (g) Liu, H. Y.; Zhou, H.; Liu, L. Y.; Ying, X.; Jiang, H. F.; Chang, C. K. *Chem. Lett.* **2007**, *36*, 274–275.

(11) (a) Bendix, J.; Golubkov, G.; Gray, H. B.; Gross, Z. *Chem. Commun.* **2000**, 1957–1958. (b) Gross, Z.; Golubkov, G.; Simkhovich, L. *Angew. Chem., Int. Ed.* **2000**, *39*, 4045–4047. (c) Meier-Callahan, A. E.; Gray, H. B.; Gross, Z. *Inorg. Chem.* **2000**, *39*, 3605–3607. (d) Meier-Callahan, A. E.; Di Bilio, A. J.; Simkhovich, L.; Mahammed, A.; Goldberg, I.; Gray, H. B.; Gross, Z. *Inorg. Chem.* **2001**, *40*, 6788–6793. (e) Golubkov, G.; Bendix, J.; Gray, H. B.; Mahammed, A.; Goldberg, I.; DiBilio, A. J.; Gross, Z. *Angew. Chem., Int. Ed.* **2001**, *40*, 2132–2134. (f) Mandimutsira, B. S.; Ramdhanie, B.; Todd, R. C.; Wang, H.; Zareba, A. A.; Czernuszewicz., R. S.; Goldberg, D. P. *J. Am. Chem. Soc.* **2002**, *124*, 15170–15171. (g) Saltsman, I.; Mahammed, A.; Goldberg, I.; Tkachenko, E.; Botoshansky, M.; Gross, Z. *J. Am. Chem. Soc.* **2002**, *124*, 7411–7420. (h) Golubkov, G.; Gross, Z. *Angew. Chem., Int. Ed.* **2003**, *42*, 4507–4509. (i) Liu, H.-Y.; Lai, T.-S.; Yeung, L.-L.; Chang, C. K. *Org. Lett.* **2003**, *5*, 617. (j) Golubkov, G.; Gross, Z. *J. Am. Chem. Soc.* **2005**, *127*, 3258–3259. (k) Mahammed, A.; Gross, Z. *J. Am. Chem. Soc.* **2005**, *127*, 2883–2884. (l) Liu, H.-Y.; Yam, F.; Xie, Y.-T.; Li, X.-Y.; Chang, C. K. *J. Am. Chem. Soc.* **2009**, *131*, 12890–12891. (m) Czernuszewicz, R. S.; Mody, V.; Czader, A.; Gatezowski, M.; Gryko, D. T. *J. Am. Chem. Soc.* **2009**, *131*, 14214–14215.

(12) Collman, J. P.; Zeng, L.; Decre'au, R. A. *Chem. Commun.* **2003**, 2974–2975.

(13) Wang, S. H.; Mandimutsira, B. S.; Todd, R.; Ramadhanie, B.; Fox, J. P.; Goldberg, D. P. *J. Am. Chem. Soc.* **2004**, *126*, 18–19.

(14) Zhang, R.; Harishchandra, D. N.; Newcomb, N. *Chem.—Eur. J.* **2005**, *11*, 5713–5720.

Chart 1

	Ar$_5$	Ar$_{10}$	Ar$_{15}$
1	C$_6$F$_5$	C$_6$F$_5$	C$_6$F$_5$
2	C$_6$F$_5$	C$_7$H$_7$O	C$_6$F$_5$
3	C$_6$H$_3$Br$_2$	C$_6$F$_5$	C$_6$H$_3$Br$_2$
4	C$_6$H$_3$F$_2$	C$_6$H$_3$F$_2$	C$_6$H$_3$F$_2$
5	C$_6$H$_3$Cl$_2$	C$_6$H$_3$Cl$_2$	C$_6$H$_3$Cl$_2$

relevant under such conditions. We now present the synthesis of five corroles that differ significantly in the steric and electronic effects of their aryl substituents (Chart 1), from which two series of manganese(III) complexes were prepared: the metal insertion products **1-Mn** to **5-Mn** and the β-pyrrole-brominated derivatives **1a-Mn** to **5a-Mn** (Chart 1). Two of the free-base corroles (**2** and **5**) and six of the manganese(III) corroles (**1-Mn**, **1a-Mn**, **3-Mn**, **5-Mn**, **5a-Mn**, [**5-Mn**]*) were also characterized by X-ray crystallography, for evaluating possible steric interactions that may affect their reactivity or stability. The Mn^{III}/(O)Mn^V transformation was performed with ozone as oxidant to avoid the problems inherent with other oxidants such as their coordination to the metal center and other interferences.[17] The as-such prepared (oxo)manganese(V) corroles are very stable at low temperature and may even be characterized at room temperature. Most valuable information regarding constitution and purity was obtained by the combination of ^{19}F and ^{1}H spectroscopy of these diamagnetic low-spin d^2 complexes. The

thermal stability of the (oxo)manganese(V) corroles allowed for investigating their reactivity, which was addressed by kinetic studies that focused on stoichiometric OAT to ring-substituted thioanisoles.

2. Experimental Section

2.1. Materials. Silica gel for column chromatography (Silica Gel 60, 63-200 μm mesh) was obtained from E. Merck Ltd. Chemicals, as were all solvents (ethyl acetate, toluene, CH$_2$Cl$_2$, hexanes, methanol, and acetonitrile). Most starting materials for syntheses were from Sigma-Aldrich and used without further purification. Exceptions are pyrrole and pentafluorobenzaldehyde, which were purified by vacuum distillation before use. Tetrabutylammonium perchlorate, which was used as a supporting electrolyte in the CV experiments, was also obtained from Fluka and used after three crystallizations. Electrodes for CV were obtained from CH Instruments. Deutrated solvents were obtained from Sigma-Aldrich.

2.2. Physical Methods. Nuclear Magnetic Resonance Spectroscopy. ^{1}H and ^{19}F NMR data were recorded on a Bruker AM 200 and AM 600 operating at 200 and 600 MHz for ^{1}H and 188 and 565 MHz for ^{19}F, respectively. ^{1}H chemical shifts are reported relative to solvent peaks CDCl$_3$ at 7.24 ppm and to CFCl$_3$ (0.00) in the ^{19}F NMR spectra.

Mass Spectrometry. Measurements were made on CH$_3$CN solutions on Micromass MS Technologies Maldi micro MX with ionization by a nitrogen laser at 337 nm.

X-ray Crystallography. The X-ray diffraction measurements were carried out on a Nonius Kappa CCD diffractometer, using graphite monochromated Mo Kα radiation (λ = 0.7107 Å).

Cyclic Voltammetry. CV measurements were made with Wave-Now USB potentiostat/galvanostat (Pine Research Instrumentation) using Pine AfterMath Data Organizer software. A three-electrode

(15) (a) Eikley, R. A.; Khan, S. I.; Abu-Omar, M. H. *Angew. Chem., Int. Ed.* **2002**, *41*, 3592–3595. (b) Edwards, N. Y.; Shields, C. E.; Loring, M. I.; Abu-Omar, M. H. *Inorg. Chem.* **2005**, *44*, 3700–3708. (c) Zdilla, M. J.; Abu-Omar, M. H. *J. Am. Chem. Soc.* **2006**, *128*, 16971–16979. (d) Zdilla, M. J.; Dexheimer, J. L.; Abu-Omar, M. H. *J. Am. Chem. Soc.* **2007**, *129*, 11505–11511.

(16) (a) Nam, W.; Han, H. J.; Oh, S. Y.; Lee, Y. J.; Choi, M. H.; Han, S. Y.; Kim, C.; Woo, S. K.; Shin, W. *J. Am. Chem. Soc.* **2000**, *122*, 8677–8684. (b) Nam, W.; Lim, M. H.; Oh, S. Y. *Inorg. Chem.* **2000**, *39*, 5572–5575. (c) Nam, W.; Lim, M. H.; Oh, S. Y.; Lee, J. H.; Lee, H. J.; Woo, S. K.; Kim, C.; Shin, W. *Angew. Chem., Int. Ed.* **2000**, *39*, 3646–3649.

(17) (a) Gross, Z.; Nimri, S. *Inorg. Chem.* **1994**, *33*, 1731–1732. (b) Czarnecki, K.; Nimri, S.; Gross, Z.; Proniewicz, L. M.; Kincaid, J. R. *J. Am. Chem. Soc.* **1996**, *118*, 2929–2935.

system consisting of a platinum wire working electrode, a platinum wire counter electrode, and an Ag/AgCl reference electrode, was employed. The CV measurements were performed using acetonitrile solutions of 0.5 M tetrabutylammonium perchlorate (TBAP, Fluka, recrystallized three times from absolute ethanol), and 10^{-3} M substrate under an argon atmosphere at ambient temperature. The scan rate was 100 mV/s, and the $E_{1/2}$ value for oxidation of ferrocene under these conditions was 0.44 V.

UV–Vis Absorption Spectroscopy. Absorption spectral measurements were recorded with an Agilent 8453 diode array spectrophotometer. Extinction coefficients were calculated from measurements on corroles at variable concentrations in ethyl acetate and dichloromethane solutions.

Ozonolyzer. Welsbach manufactured ozonolyzer was used to produce O_3 by passing O_2 through an electricity arc.

Refrigerated Bath Circulator. An M.R.C. Ltd. refrigerated bath circulator, BL-30, was used to maintain stable temperatures for the kinetic measurements.

Stopped-Flow Spectrophotometer. Fast kinetics experiments were performed using an Applied Photophysics PiStar-180 spectrometer in photomultiplier mode.

2.3. Syntheses of Free-Base Corroles. 5,10,15-Tris-pentafluorophenylcorrole (**1**), 5,15-bis-pentafluorophenyl-10-*p*-methoxyphenylcorrole (**2**), 5,15-bis-(dibromophenyl)-10-pentafluorophenylcorrole (**3**), 5,10,15-tris-difluorophenylcorrole (**4**), and 5,10,15-tris-dichlorophenylcorrole (**5**) were prepared by procedures reported in the literature.[8,9,18]

2.4. Synthesis of Manganese(III) Corroles. The manganese(III) triarylcorroles, as well as the β-pyrrole-brominated complexes, were synthesized similar to previously published procedures, as outlined below.[11b,n]

Synthesis of 5,10,15-Tris-(pentafluorophenyl)corrolato–Manganese(III), 1-Mn. H₃tpfc (50 mg, 63 μmol) and manganese acetate tetrahydrate (154 mg, 630 μmol) were dissolved in DMF and heated for reflux for 10 min. The solution changed color from purple to green, and the reaction progress was monitored by TLC (silica, hexane/CH₂Cl₂ = 4:1) until the starting material disappeared. The resulting solution was evaporated to dryness, dissolved in CH₂Cl₂ with silica gel, followed by column chromatography (silica gel, hexane/ethyl acetate = 10:1 eluent) and isolation of the green complex. Recrystallization from hot *n*-hexane provided purple needle-shaped crystals (48.8 mg, 91%). **1-Mn**, UV–visible (CH₂Cl₂) λ_{max}(log ε): 400(4.62), 416(4.64), 482(4.29), 600 (4.1). MS (MALDI-TOF LD⁺): m/z (%) = 848.0 [M]⁺ (100).

Synthesis of 5,10-Bis-pentafluorophenyl-15-*p*-anisylcorrolato–Manganese(III), 2-Mn. This corrole was similarly prepared following the same procedure as **1-Mn** in 90% yield. **2-Mn**: UV–vis (CH₂Cl₂) λ_{max}(log ε): 401(4.5), 424(4.4), 491(4.2), 600(3.9). MS (MALDI-TOF LD⁺): m/z (%) = 788.2 [M]⁺ (100).

Synthesis of 5,10-Bis-(2,6-dibromophenyl)-15-pentafluorophenylcorrolato–Manganese(III), 3-Mn. This corrole was similarly prepared following the same procedure as **1-Mn** in 90% yield. **3-Mn**: UV–vis (CH₂Cl₂) λ_{max}(log ε): 403(4.5), 424(4.4), 487(4.3), 600(3.9). MS (MALDI-TOF LD⁺): m/z (%) = 983.8 [M]⁺ (100).

Synthesis of 5,10,15-Tris-(2,6-difluorophenyl)corrolato–Manganese(III), 4-Mn. This corrole was similarly prepared following the same procedure as **1-Mn** in 90% yield. **4-Mn**: UV–vis (CH₂Cl₂) λ_{max}(log ε): 399(4.5), 420(4.5), 488(4.1), 600(3.9). MS (MALDI-TOF LD⁻): m/z (%) = 685.0 [M – H]⁻ (100).

Synthesis of 5,10,15-Tris-(2,6-dichlorophenyl)corrolato–Manganese(III), 5-Mn. This corrole was similarly prepared following the same procedure as **1-Mn** in 90% yield. **5-Mn**: UV–vis (CH₂Cl₂) λ_{max}(log ε): 403(4.6), 424(4.5), 494(4.1), 600(4.0). MS (MALDI-

(18) For a detailed discussion of the NMR properties of corroles see: (a) Balazas, Y. S.; Saltsman, I.; Mahammed, A.; Tkachenko, E.; Golubkov, G.; Levine, J.; Gross, Z. *Magn. Reson. Chem.* **2004**, *42*, 624–635. (b) Etinger, I.; Kumar, A.; Gross, Z. Unpublished results.

TOF): m/z (%) = 782. Six [M – H]⁻ (50%), 825.86 [M + CH₃CN]⁻ (100%).

Synthesis of 2,3,7,8,12,13,17,18-Octabromo-5,10,15-tris(pentafluorophenyl)corrolato–Manganese(III), 1a-Mn. 1-Mn (10 mg, 11.8 μmol) was dissolved in 5 mL of methanol. A solution of approximately 100 equiv (1.18 mmol) of Br₂ in methanol was added dropwise to this solution. The color of the solution first changed from green to brown but became green again later. The reaction mixture was stirred overnight at room temperature. The excess Br₂ was evaporated by a stream of nitrogen gas. The resulting green solution was evaporated at room temperature. Column chromatography (silica gel, 10:1 hexane/ethyl acetate) provided a purple powder of **1a-Mn** (14.8 mg, 85%). **1a-Mn**: UV–vis (CH₂Cl₂) λ_{max}(log ε): 402(4.7), 422(4.6), 490(4.4), 612(4.2). MS (MALDI-TOF LD⁻): m/z (%) = 1558.7 [M + Br]⁻ (100), 1479.7 [M]⁻ (70).

Synthesis of 2,3,7,8,12,13,17,18-Octabromo-5,10-bispentafluorophenyl-15-*p*-anisylcorrolato–Manganese(III), 2a-Mn. This corrole was also prepared following the same procedure as **1a-Mn** in 85% yield. **2a-Mn**: UV–vis (CH₂Cl₂) λ_{max}(log ε): 402(4.8), 425(4.7), 501(4.5), 616(4.2). MS (MALDI-TOF LD⁻): m/z (%) = 1418.1 [M – H]⁻ (100), 1499.4 [M + Br]⁻ (90).

Synthesis of 2,3,7,8,12,13,17,18-Octabromo-5,10-bis(2,6-dibromophenyl)-15-pentafluorophenyl-corrolato–Manganese(III), 3a-Mn. This corrole was also prepared following the same procedure as **1a-Mn** in 65% yield. **3a-Mn**: UV–vis (CH₂Cl₂) λ_{max}(log ε): 408(4.3), 505(4.1), 431(4.2), 616(3.8). MS (MALDI-TOF LD⁺): m/z (%) = 1615.2 [M]⁺ (100), 1535.3 [M – Br]⁺ (30), 1455.3 [M – 2Br]⁺ (20).

Synthesis of 2,3,7,8,12,13,17,18-Octabromo-5,10,15-tris(2,6-difluorophenyl)corrolato–Manganese(III), 4a-Mn. This corrole was also prepared following the same procedure as **1a-Mn** in 60% yield. **4a-Mn**: UV–vis (CH₂Cl₂) λ_{max}(log ε): 406(4.9), 427(4.8), 505(4.5), 616(4.3). MS (MALDI-TOF LD⁻): m/z (%) = 1317.5 [M]⁻ (80), 1398.5 [M + Br]⁻ (100).

Synthesis of 2,3,7,8,12,13,17,18-Octabromo-5,10,15-tris(2,6-dichlorophenyl)corrolato–Manganese(III), 5a-Mn. This corrole was also prepared following the same procedure as that for **1a-Mn** in 80% yield. **5a-Mn**: UV–vis (CH₂Cl₂) λ_{max}(log ε): 410(4.6), 432(4.5), 511(4.2), 616(4.1). MS (MALDI-TOF LD⁻): m/z (%) = 1496.4 [M + Br]⁻ (100), 1415.4 [M]⁻ (70), 1450.4 [M + Cl]⁻ (30).

2.5. Synthesis of (Oxo)manganese(V) Corroles. Stock solutions (14.7 μM) of manganese(III) corroles (**1-Mn** to **5-Mn** and **1a-Mn** to **5a-Mn**) were prepared in a volumetric flask. 2.5-mL aliquots were flushed by a slow stream of ozone in a dry ice/acetone bath until the color changed from green to red or brown, for **1-Mn(O)** to **5-Mn(O)** and **1a-Mn(O)** to **5a-Mn(O)**, respectively. The excess amount of ozone was flushed away with a stream of argon, and these solutions were used for the kinetic experiments. The same procedures, but with 3–4 mg of manganese(III) corroles in deutrated solvents was used for NMR-based structural characterization.

1-Mn(O): MS (ES⁺) (%). 864.96 [M + H]⁺ (100), 889.01 [M + Na]⁺. UV–vis(EtOAc) λ_{max}[nm] (relative %): 347(100), 404(77), 518(20). ¹H NMR (CDCl₃): δ = 9.5 (br s, 2H), 9.2 (d, J = 4.1 Hz, 2H), 9.03(d, J = 4.6 Hz, 2H), 8.9 (d, J = 4.7 Hz, 2H): ¹⁹F NMR (CDCl₃): δ = −131.9 (d, J = 22.2 Hz, 2F), −132.3 (d, J = 22.3 Hz, 1F), −132.5 (d, J = 22.9 Hz, 2F), −133.1(d, J = 21.6 Hz, 1F), −146.5 (t, J = 21.5 Hz, 2F), −146.6 (t, J = 21.2 Hz, 1F), −155.8 (m, 6F).

2-Mn(O): MS (ES⁺) (%). 788.02 [M − O]⁺ (20), 804.02 [M]⁺ (20), 829.02 [M − O + CH₃CN]⁺ (100). UV–vis (EtOAc) λ_{max}[nm] (relative %): 349(100), 408(85), 518(18). ¹H NMR (CDCl₃): δ = 9.5 (br s, 2H), 9.2 (d, J = 4.2 Hz, 2H), 9.1(d, J = 4.8 Hz, 2H), 8.9 (d, J = 4.6 Hz, 2H), 8.1 (d, J = 8.1 Hz, 1H), 8.0(d, J = 8.4 Hz, 1H), 7.4(d, J = 8.2 Hz, 1H), 7.3(d, J = 8.2 Hz, 1H), 4.1 (s, 3H): ¹⁹F NMR (CDCl₃): δ = −132.0 (d, J = 24.2 Hz, 2F), −132.8 (d, J = 24.2 Hz, 2F), −147.2 (t, J = 20.8 Hz, 2F), 156.1 (t, J = 23.7 Hz, 2F), −156.2 (t, J = 21.3 Hz, 2F).

3-Mn(O): MS (ES$^+$) (%). 999.69 [M]$^+$ (100), 1024.75 [M + Na]$^+$. UV−vis (EtOAc) λ_{max}[nm] (relative %): 349(100), 409(85), 518(20). ^{1}H NMR (CDCl$_3$): δ = 9.4 (d, J = 4.6 Hz, 2H), 9.01 (d, J = 4.5 Hz, 2H), 8.84(overlapping of two doublets, 4H), 8.1 (d, J = 8.4 Hz, 2H), 8.0 (d, J = 8.3 Hz, 2H), 7.6(t, J = 8.4 Hz, 2H): ^{19}F NMR (CDCl$_3$): δ = −132.0 (d, J = 23.4 Hz, 1F), −132.5 (d, J = 23.4 Hz, 1F), −147.4 (t, J = 22.0 Hz, 1F), 156.3 (t, J = 20.8 Hz, 1F), −156.7 (t, J = 22.0 Hz, 1F).

4-Mn(O): MS (ES$^+$) (%). 702.82 [M + H]$^+$ (50), 685.83 [M − O]$^+$ (20), 726.85 [M + Na]$^+$ (100). UV−vis (EtOAc) λ_{max}[nm] (relative %): 347(100), 405(79), 518(18).). ^{1}H NMR (CDCl$_3$): δ = 9.41 (d, J = 4.4 Hz, 2H), 9.18 (d, J = 4.3 Hz, 2H), 8.99 (d, J = 4.8 Hz, 2H), 8.93 (d, J = 4.7 Hz, 2H), 7.45−7.82 (m, 9H). ^{19}F NMR (CDCl$_3$): δ = −104.3 (br s, 2F), −104.8 (br s, 1F), −105.09 (br s, 2F), −105.4(br s, 2F).

5-Mn(O): MS (ES$^+$) (%). 799.84 [M]$^+$ (100), 824.89 [M + Na]$^+$ (50). UV−vis (EtOAc) λ_{max} [nm] (relative %): 347(100), 405(83), 518(19). ^{1}H NMR (CDCl$_3$): δ = 9.36 (d, J = 4.5 Hz, 2H), 9.01 (d, J = 4.4 Hz, 2H), 8.77 (d, J = 4.8 Hz, 2H), 8.73 (d, J = 4.7 Hz, 2H), 7.89 (d, J = 7.7 Hz, 4H), 7.85 (d, J = 8.1 Hz, 2H) 7.76−7.89 (m, 9H).

1a-Mn(O): UV−vis (CH$_2$Cl2) λ_{max}[nm] (relative %): 388(100), 421(83), 537(23). ^{19}F NMR (CDCl$_3$): δ = −132.3 (two ovelaping doublets, 3F), −132.6 (two ovelaping doublets, 3F), 146.1 (t, J = 20.7 Hz, 2F), −146.2 (t, J = 20.7 Hz, 1F), −157.7 (m, 6F).

2a-Mn(O). UV−vis (CH$_2$Cl$_2$) λ_{max}[nm] (relative %): 373(85), 416(100), 534(100). ^{1}H NMR (CDCl$_3$): δ = 7.9 (d, J = 7.8 Hz, 1H), 7.6 (d, J = 7.7 Hz, 1H), 7.3 (dd, J = 7.5 Hz, 2H), 7.6 (d, J = 7.3 Hz, 1H), 4.1 (s, 3H)): ^{19}F NMR (CDCl$_3$): δ = −132.5 (d, J = 23.1 Hz, 2F), −132.8 (d, J = 23.1 Hz, 2F), −146.7 (t, J = 20.8 Hz, 2F), −157.9 (m, 4F).

3a-Mn(O): MS (ES$^+$) (%). 1632.33 [M + H]$^+$ (25), 1656.33 [M − O + CH$_3$CN]$^+$ (80), 1670.35 [M + CH$_3$CN]$^+$ (60), 1706.36 [M − O + Br]$^+$ (100). UV−vis (CH$_2$Cl$_2$) λ_{max}[nm] (relative %): 392(97), 425(100), 537(20). ^{1}H NMR (CDCl$_3$): δ = 7.9 (d, J = 8.3 Hz, 2H), 7.3 (d, J = 8.3 Hz, 2H), 7.5(t, J = 8.3 Hz, 2H): ^{19}F NMR (CDCl$_3$): δ = −131.8 (d, J = 23.6 Hz, 1F), −132.6 (d, J = 22.7 Hz, 1F), −147.4 (t, J = 21.9 Hz, 1F), 157.6 (m, 2F).

4a-Mn(O): UV−vis (CH$_2$Cl$_2$) λ_{max}[nm] (relative %): 391(100), 423(100), 537(30). ^{1}H NMR (CDCl$_3$): δ = 7.53−766 (m, 9H). ^{19}F NMR (CDCl$_3$): δ = −104.9 (br s, 1F), −105.1 (br s, 2F), −105.2 (br s, 2F), −105.5(br s, 1F).

5a-Mn(O). MS (ES$^+$) (%). 1431.29 [M]$^+$ (40), 1456.34 [M − O + CH$_3$CN]$^+$ (100), 1484.61 [M − O − Br]$^+$ (50). UV−vis (CH$_2$Cl$_2$) λ_{max}[nm] (relative %): 387(97), 422(100), 537(19). ^{1}H NMR (CDCl$_3$): δ = 7.69−7.73 (m, 9H).

2.6. Crystallography. X-ray quality crystals of **2** were grown in hexane at low temperature (−4 °C) and **5** in a 1/1 mixture of dichloromethane/hexane at room temperature. For all manganese(III) corroles, **1-Mn**, **1a-Mn**, **3-Mn**, **5-Mn**, and **5a-Mn**, single crystals of X-ray quality were grown in ethylacetate/hexane mixtures at room temperature. **[5-Mn]*** was obtained by growing crystals in the presence of phenylmethylsulfoxide. Methods of crystal mounting and data analysis are identical to those of previous reports.[11g]

2.7. Crystal Data: 2. C$_{38}$H$_{17}$F$_{10}$N$_4$O, M = 735.56, triclinic, space group P$\bar{1}$, a = 15.0003(3) Å, b = 16.0686(2) Å, c = 16.5517(3) Å, α = 67.4337(6)°, β = 64.9752(6)°, γ = 75.281(6)°, V = 3406.59(10) Å^3, Z = 4, T = 110(2) K, D_c = 1.436 g/cm^3, μ(MoKα) = 0.126 mm^{-1}, 15948 unique reflections to θ_{max} = 27.84°, 957 refined parameters, R_1 = 0.058 for 8352 observations with $I > 2\sigma(I)$, wR_2 = 0.162 for all data.

5: C$_{37}$H$_{20}$F$_6$N$_4$, M = 634.57, monoclinic, space group P2$_1$/c, a = 17.911(4) Å, b = 12.858(3) Å, c = 13.559(3) Å, β = 110.68(3)°, V = 2921.4(11) Å^3, Z = 4, T = 293(2) K, D_c = 1.443 g/cm^3, μ(Mo Kα) = 0.113 mm^{-1}, 5309 unique reflections to θ_{max} = 25.32°, 433 refined parameters, R_1 = 0.057 for 2785 observations with $I > 2\sigma(I)$, wR_2 = 0.162 for all unique data.

1-Mn: C$_{41}$H$_{16}$F$_{15}$MnN$_4$O$_2$, M = 936.52, monoclinic, space group P2$_1$/c, a = 14.816(3) Å, b = 39.268(8) Å, c = 7.422(1) Å, β = 104.29(3)°, V = 4184.5(13) Å^3, Z = 4, T = 180(2) K, D_c = 1.487 g/cm^3, μ(Mo Kα) = 0.422 mm^{-1}, 7086 unique reflections to θ_{max} = 25.00°, 568 refined parameters, R_1 = 0.096 for 5515 observations with $I > 2\sigma(I)$, wR_2 = 0.280 for all unique data. (this structure determination is characterized by relatively low precision due to poor-quality crystals and the obtained diffraction data).

1a-Mn: C$_{41}$H$_8$Br$_8$F$_{15}$MnN$_4$O$_2$, M = 1567.73, monoclinic, space group P2$_1$/c, a = 23.2370(10) Å, b = 7.4218(4) Å, c = 32.1102(16) Å, β = 104.732(2)°, V = 5274.6(4) Å^3, Z = 4, T = 110(2) K, D_c = 1.974 g/cm^3, μ(Mo Kα) = 6.401 mm^{-1}, 9433 unique reflections to θ_{max} = 25.30°, 642 refined parameters, R_1 = 0.054 for 5291 observations with $I > 2\sigma(I)$, wR_2 = 0.136 for all unique data.

3-Mn: C$_{41}$H$_{22}$Br$_4$F$_5$MnN$_4$O$_2$, M = 1072.21, orthorhombic, space group P2$_1$2$_1$2$_1$, a = 11.7695(2) Å, b = 16.4116(3) Å, c = 19.4712(2) Å, V = 3760.99(3) Å^3, Z = 4, T = 110(2) K, D_c = 1.894 g/cm^3, μ(Mo Kα) = 0.719 mm^{-1}, 8859 unique reflections to θ_{max} = 27.88°, 516 refined parameters, R_1 = 0.033 for 7658 observations with $I > 2\sigma(I)$, wR_2 = 0.075 for all unique data.

5-Mn: C$_{45}$H$_{33}$Cl$_6$MnN$_4$O$_4$, M = 961.39, orthorhombic, space group Pbcn, a = 38.806(8) Å, b = 15.342(3) Å, c = 14.647(3) Å, V = 8720(3) Å^3, Z = 8, T = 293(2) K, D_c = 1.465 g/cm^3, μ(Mo Kα) = 0.719 mm^{-1}, 7608 unique reflections to θ_{max} = 25.02°, 529 refined parameters, R_1 = 0.062 for 4214 observations with $I > 2\sigma(I)$, wR_2 = 0.187 for all unique data.

5a-Mn: C$_{41}$H$_8$Br$_8$Cl$_6$MnN$_4$O$_2$, M = 1504.51, monoclinic, space group P2$_1$/n, a = 11.1966(2) Å, b = 18.4159(3) Å, c = 24.8914(6) Å, β = 99.9206(6)°, V = 5055.75(17) Å^3, Z = 4, T = 110(2) K, D_c = 1.977 g/cm^3, μ(Mo Kα) = 6.940 mm^{-1}, 11956 unique reflections to θ_{max} = 27.85°, 561 refined parameters, R_1 = 0.045 for 8794 observations with $I > 2\sigma(I)$, wR_2 = 0.109 for all unique data.

[5-Mn]*: C$_{44}$H$_{25}$Cl$_6$MnN$_4$OS, M = 925.38, monoclinic, space group P2$_1$/c, a = 12.6988(2) Å, b = 13.4937(2) Å, c = 22.5901(5) Å, β =95.0013(7)°, V = 3856.16(12) Å^3, Z = 4, T = 110(2) K, D_c = 1.594 g/cm^3, μ(Mo Kα) = 0.856 mm^{-1}, 7875 unique reflections to θ_{max} = 26.37°, 525 refined parameters, R_1 = 0.055 for 4502 observations with $I > 2\sigma(I)$, wR_2 = 0.168 for all unique data.

2.8. Kinetic Experiments. Kinetic experiments were carried out on an Agilent 8453 diode array spectrophotometer for the nonbrominated manganese corroles **1-Mn(O)** to **5-Mn(O)**. The measurements were performed in ethyl acetate as solvents and monitored by UV−vis spectroscopy. The (oxo)manganese(V) corroles were prepared by ozone oxidation of (corrolato)manganese(III) [14.7 μM in 200 mL of ethyl acetate] solutions. For each measurement, the (oxo)manganese(V) complex was freshly generated. The kinetic measurements were repeated three times for each concentration, and several wavelengths were measured. The wavelengths that differ the most between (corrolato)manganese(III) and (oxo)manganese(V) are 347, 482−490, and 600 nm. The substrate solutions were prepared by dissolving thioanisole derivative in ethyl acetate. The substrate concentrations taken for each measurement are presented in the Table S1 (Supporting Information). GC analysis of reaction mixtures confirmed the formation of the corresponding sulfoxides.

Reactions performed with **1a-Mn(O)** to **5a-Mn(O)** were much too fast to be measured by conventional mixing. Hence, their reactions with thioanisoles were examined by the stopped-flow technique. One syringe contained substrate in dichloromethane, and the other contained a solution of (oxo)manganese(V) corroles in dichloromethane. Equal volumes were injected into the stopped-flow cell. The constant temperature (20 °C) was assured by the instrument configuration: water from a thermostatted bath over the flow path and the firing syringes filled with reagents.

Determination of the Reaction Constants for the Reactions of (Oxo)manganese(V) Corroles with Thioanisoles. The oxygen transfer reactions were followed by UV−vis spectroscopy by examining changes in absorbance by time. The reactions were performed in ethyl acetate at 20 °C. The concentrations of

thioanisoles were at least 1000 times more concentrated than the solution of (oxo)manganese(V) corrole. Each reaction was scanned in the wavelength range of 300−700 nm and repeated three times. Pseudo-first-order rate constants (k_{obs}) were obtained from the changes in absorbance at several wavelengths: disappearance of (oxo)manganese(V) mostly at 347 and 410 nm, and appearance of manganese(III) corroles mostly at 482−490 and 600 nm. All the reactions displayed typical pseudo-first-order behavior.

3. Results and Discussion

3.1. Synthesis. The large advances in the synthesis of 5,10,15-triarylcorroles (unknown prior to 1999)[8] allowed for the structure/activity studies that are presented here. The current focus was on new aryl substituents that may induce electronic effects (5 F atoms in each aryl ring of **1** vs only 2 in **4**, a C_{10} anisyl group in **2** vs a $C_{10}-C_6F_5$ group in **1**, etc.) and steric demands (2 Br atoms in **3** vs 2 Cl atoms in **5**, for example). The series of free-base corroles (**1−5**) was prepared by currently established methods,[8,9] characterized by NMR (^{1}H and ^{19}F), UV−visible and mass spectroscopy; the data were matched with previous literature.[8,9,18] Synthesis of a corrole with three 2,6-dibromophenyl *meso*-substituents was attempted as well, but this particular derivative is not accessible by any of the currently available synthetic methodologies.[9e] Insertion of manganese into **1−5** was easily achieved by heating their DMF solutions with manganese acetate tetrahydrate, thus completing the synthetic route for **1-Mn** to **5-Mn**. The second series of complexes was obtained by reacting **1-Mn** to **5-Mn** with excess bromine, from which the β-pyrrole-brominated **1a-Mn** to **5a-Mn** complexes were isolated in high yields. This previously published route for **1a-Mn** worked equally well for gaining access to the new β-pyrrole-brominated derivatives **2-Mn** to **5-Mn**.[11b] The brominated (**1a-Mn** to **4a-Mn**) and nonbrominated (**1-Mn** to **4-Mn**) complexes are stable at room temperature in the solid state, as well as in solution, but **2-Mn** and **2a-Mn** (both contain a C_{10} anisyl group) are only stable in solution for a short time and gradually developed an orange-colored spot in TLC. The oxidation to the corresponding (oxo)manganese(V) derivatives was achieved by passing ozone into solutions of the corresponding manganese(III) corroles, upon which the color changed from green to either red [**1-Mn(O)** to **5-Mn(O)**] or brown [**1a-Mn(O)** to **5a-Mn(O)**]. Other oxidants like PhIO and m-CPBA may also be used to produce oxo-species,[12,13] but ozone is preferable because its only byproduct is O_2 and this allows for much more straightforward characterization than in cases where either the oxidant or its product may coordinate to the metal.[17] The thus produced (oxo)manganese(V) complexes are very stable in dilute solutions (μM to mM) at room temperature, but more concentrated solutions are only stable at low temperatures. Two exceptions are **2-Mn(O)**, which is of limited stability even at low temperature, and **5-Mn(O)**, which is particularly stable, thus allowing its isolation as a solid at room temperature. The brominated (oxo)manganese(V) complexes [**1a-Mn(O)** to **5a-Mn(O)**] are significantly more stable than the nonbrominated analogues [**1-Mn(O)** to **5-Mn(O)**], which may be safely attributed to the reduced oxidation-sensitivity of C−Br vs C−H bonds.

3.2. Structural Elucidation. 3.2.1. UV−Visible Spectroscopy. The electronic spectra of manganese(III) corroles are similar to those of previously reported manganese(III) porphyrins and corroles.[3−6,10,11] They display split Soret bands ($\lambda_{max} = 400−425$ nm), a ligand-sensitive absorbance at $\lambda_{max} = 480−490$
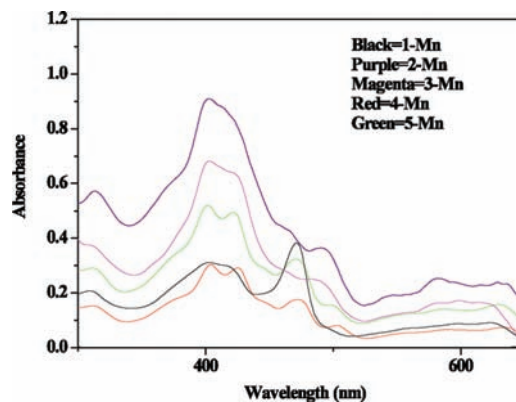

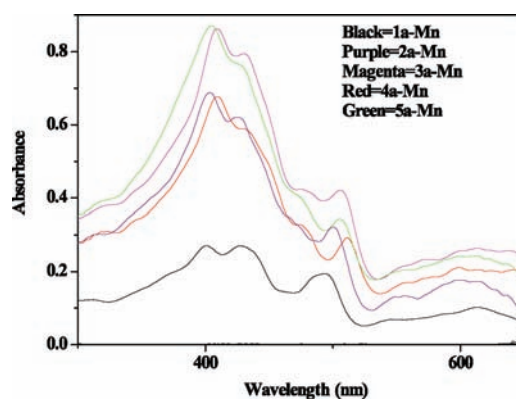**Figure 1.** UV−vis spectra of manganese(III) corroles **1-Mn** to **5-Mn**, in ethyl acetate.

Figure 2. UV−vis spectra of β-pyrrole-brominated manganese(III) corroles **1a-Mn** to **5a-Mn**, in ethyl acetate.
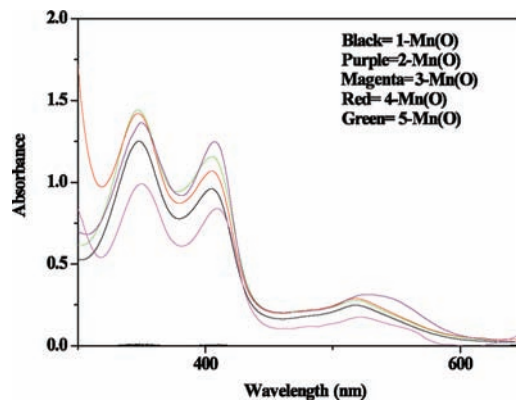

Figure 3. UV−vis spectra of (oxo)manganese(V) corroles **1-Mn(O)** to **5-Mn(O)**, in ethyl acetate.

nm and broad Q bands at 600 nm (Figure 1).[19] The electronic spectra of the octabrominated derivatives **1a-Mn** to **5a-Mn** are similar in shape, but with significantly red-shifted (10−20 nm) Soret bands and Q bands (Figure 2). The electronic spectra of the (oxo)manganese(V) complexes are remarkably different: they display split Soret bands in the region of 347−410 nm and one broad Q-band at about 520 nm for **1-Mn(O)** to **5-Mn(O)** (Figure 3). The spectra of the **1a-Mn(O)** to **5a-Mn(O)** complexes are similar in shape, but significantly red-shifted (Figure 4).

3.2.2. NMR Spectroscopy. The free-base corroles were characterized by their ^{1}H and ^{19}F NMR and the data was either

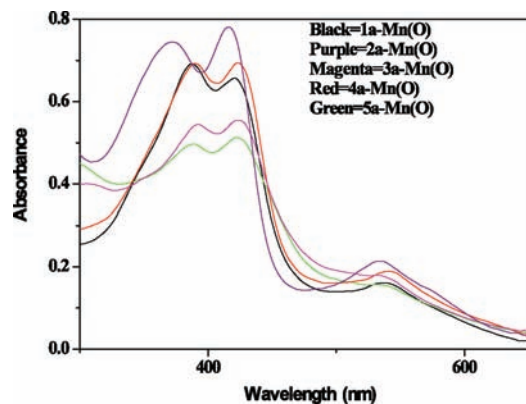(19) Boucher, L. J. *Ann. N.Y. Acad. Sci.* **1973**, *206*, 409−419.

Figure 4. UV−vis spectra of β-pyrrole-brominated (oxo)manganese(V) corroles **1a-Mn(O)** to **5a-Mn(O)**, in dichloromethane.
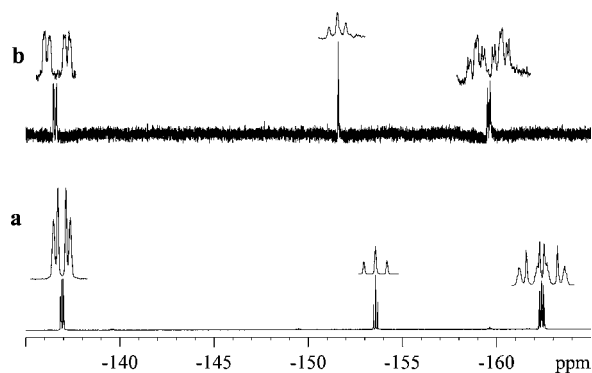

Figure 5. ^{19}F NMR spectra (room temperature, CD$_3$CN) of (a) the free-base corrole **3** and (b) the (oxo)manganese(V) corrole **3-Mn(O)**.
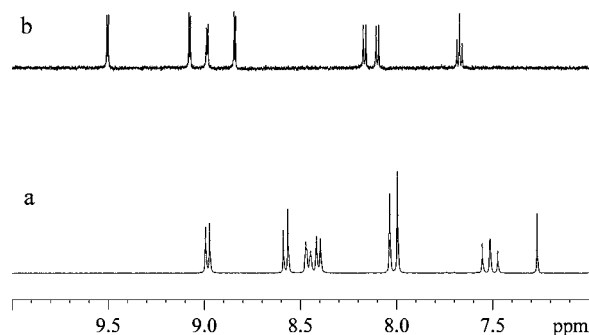

Figure 6. ^{1}H NMR spectra (room temperature, CD$_3$CN) of (a) the free base corrole **3** and (b) the (oxo)manganese(V) corrole **3-Mn(O)**.

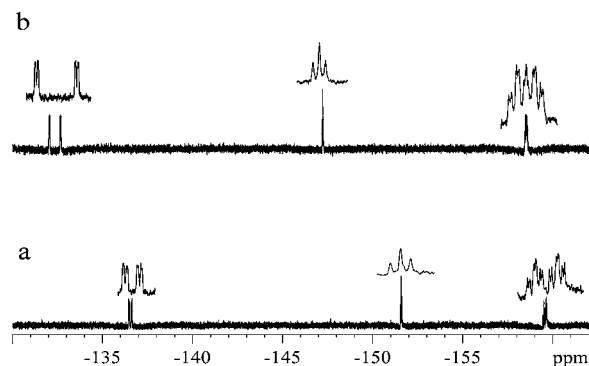**Figure 7.** ^{19}F NMR spectra (room temperature) of (a) **3-Mn(O)** in CD$_3$CN and (b) **3a-Mn(O)** in CDCl$_3$.
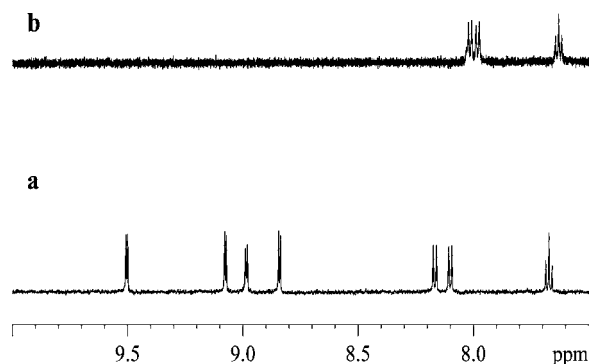

Figure 8. ^{1}H NMR spectra (room temperature) of (a) **3-Mn(O)** in CD$_3$CN and (b) **3a-Mn(O)** in CDCl$_3$.

matched with reported literature or analyzed by well described procedures.[8,9,18] The manganese(III) corroles were not characterized by NMR due to their paramagnetism, but the ^{1}H NMR spectra of the (oxo)manganese(V) corroles display sharp resonances at chemical shifts that are similar to the corresponding free-base corroles. The well-resolved signals in both the ^{1}H and ^{19}F NMR spectra demonstrate that **1-Mn(O)** to **5-Mn(O)** and **1a-Mn(O)** to **5a-Mn(O)** complexes are authentic d^2 low-spin diamagnetic species.[11] The main features are presented for two representative complexes, **3-Mn(O)** and **3a-Mn(O)**, while the spectra of all other complexes are provided as Supporting Information. The two o-F atoms of the sole C$_6$F$_5$ ring (on C$_{10}$) in the free-base corrole **3** are identical and characterized by a dd ($^1J = 23.8$ Hz and $^2J = 8.3$ Hz) coupling pattern at −136.8 ppm. In **3-Mn(O)**, however, they split into two kinds of o-F at −136.6 ppm and −136.5 ppm (both are doublets with $J = 22.8$ Hz) (Figure 5).[18a] This confirms that the manganese ion is 5-coordinated, thus inducing the nonequivalence of o-F atoms that are *syn* and *anti* to the [M(O)]$^{+3}$ moiety (a triple metal to oxygen bond). The ^{1}H NMR spectrum of **3-Mn(O)** also displays sharp resonances, which are only somewhat downfield-shifted relative to **3** (Figure 6). The ^{19}F NMR spectrum of **3a-Mn(O)** (Figure 7) may be analyzed as was **3-Mn(O)**, but its ^{1}H NMR (Figure 8) spectrum revealed only the protons from the 2,6-dibromophenyl substituents and no β-pyrrole-H (proving that all CH bonds in **3-Mn** were brominated upon its transformation to **3a-Mn**). Concluding, the NMR spectra of the ozone-oxidized manganese(III) corroles are fully consistent with the following structural and electronic features: they are manganese(V) complexes chelated by four σ-donating nitrogen atoms from the corrole and a triply bound oxygen atom (a d$_{z^2}$/p$_z$ σ bond and

two π bonds, d$_{xz}$/p$_x$ and d$_{yz}$/p$_y$) in the axial position. The two metal-based electrons are paired and reside in the only orbital that is neither σ- nor π-bonding (i.e., a (d$_{xy}$)^2 electronic state).

3.2.3. X-ray Crystallography. The free-base corroles **2** and **5**, as well as the manganese(III) complexes **1-Mn**, **1a-Mn**, **3-Mn**, **5-Mn**, and **5a-Mn**, were subjected to crystal structure analysis. In the Mn−corroles, ethyl acetate from the crystal growing solutions was found to coordinate axially to the metal centers. Further crystallization of **5-Mn** in the presence of phenylmethylsulfoxide led to preferred axial coordination of the latter to the manganese (instead of ethyl acetate) in compound **[5-Mn]***.

Only a few crystal structures of free-base corroles, including H$_3$tpfc (**1**), have been reported thus far.[8b,20] The molecular structures of all these corroles exhibit a significant distortion from planarity of the corrole macrocycle in order to minimize the steric hindrance between the three inner NH protons. This
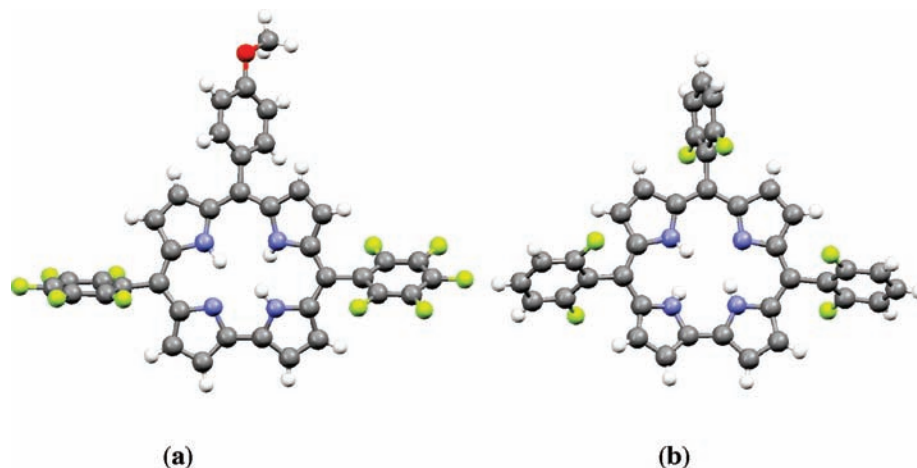
Figure 9. Molecular structures of (a) 5,10-bispentafluorophenyl-15-*p*-anisylcorrole, **2** and (b) 5,10,15-tris(2,6-difluorophenyl)corrole, **5**.

is achieved by adopting a puckered conformation in which the pyrrole rings are tilted slightly either up or down from a coplanar orientation. The same trend has been observed in this study for **2** and **5** (Figure 9). The twist angles between adjacent pyrroles on moving from ring A to D around the macrocycle are: 8.2, 20.1, 11.0, and 7.2° in **2**, and 21.4, 8.7, 3.2 and 6.5° in **5**. As a result, the NH protons (the low-temperature analysis allowed their location from diffraction data) of the A, B, and D pyrroles (see Chart 1) deviate from the mean plane of the corrole-core atoms by 0.42, 0.65, and 0.12 Å in **2**, and −0.81, −0.23, and 0.46 Å in **5**, the nonbonding distances between them inside the core exceeding the "collision" value of 2.0 Å (H···H = 2.0−2.4 Å).

Crystal structures of manganese complexes without axial ligation are rare, and the previously reported structure of **1-Mn** was obtained with triphenylphosphine oxide as an axial ligand.[11a] Our attempts to avoid axial ligation to the manganese center by using solvents of weaker coordination affinity (a mixture of ethyl acetate and hexane) were unsuccessful, and the ethyl acetate ligand was incorporated in the **1-Mn**, **1a-Mn**, **3-Mn**, **5-Mn**, and **5a-Mn** compounds. The observed structure of [**1-Mn**(EtOAc)] is thus characterized by a square-pyramidal geometry, where the manganese(III) ion is situated 0.28 Å above the mean plane of the corrole macrocycle, and 0.23 Å above the N$_4$-plane of the four pyrrole atoms. This is in agreement with other five-coordinate square-pyramidal complexes reported earlier, [(tpfc)Mn(OPPh$_3$)][11a] and [(OEC)Mn(py)].[21] In this respect, [**1-Mn**(EtOAc)] is different, however, from the structure of the square-planar [(DMHEC)Mn] complex, which in the absence of any axial ligand, is characterized by a planar geometry of the Mn−corrole macrocycle.[22] Evidently, upon complexation with manganese the corrole macrocycle adopts a much less distorted conformation than in the free-base compounds. The geometric parameters for all the crystallographically

Table 1. Bond Length Distances (in Å) and Angles (deg) in Manganese(III) Triaryl Corroles

complex	Mn−N^a	Mn−O^b	Δ(core)^c	Δ(N$_4$)^d	dihedral angles^e 5	10	15
1-Mn	1.916	2.198	0.28	0.23	77.1	82.8	76.7
1a-Mn	1.929	2.153	0.25	0.22	90.0	83.9	87.9
3-Mn	1.909	2.199	0.29	0.24	77.1	82.8	89.4
5-Mn	1.908	2.214	0.28	0.25	80.9	87.0	75.4
5a-Mn	1.926	2.253	0.17	0.13	89.3	88.5	78.7
[5-Mn]*	1.913	2.127	0.34	0.28	79.4	81.5	89.4

^{a} Average bond length. ^{b} Distance of the manganese ion from the coordinated axial ligand (ethyl acetate or phenylmethylsulfoxide). ^{c} Distance of the manganese ion from the mean plane of corrole macrocycle. ^{d} Distance of the manganese ion from the mean plane of the four pyrrole N-atoms. ^{e} Dihedral angles between the mean planes of the corrole macrocycle and the aryl rings at the respective 5-, 10-, and 15-positions.

analyzed compounds are given in Table 1, revealing typical Mn−N$_{pyrrole}$ and Mn−O$_{axial-ligand}$ coordination distances within 1.91−1.93 Å and 2.1−2.3 Å, respectively, and deviations of the manganese from the mean plane of the core ring toward the axial ligand.

Bromination on β-pyrrole carbon atoms appears to have some subtle effect on the metal coordination parameters, as the average Mn−N$_{pyrrole}$ bond length in [**1-Mn**(OEtAc)], [**3-Mn**(O-EtAc)], and [**5-Mn**(OEtAc)] is consistently shorter (by 0.01−0.03 Å) than in [**1a-Mn**(OEtAc)] and [**5a-Mn**(OEtAc)]. This may be attributed to the decreased electron density on the pyrrole N-atoms due to the electronegative β-substituents. The [**5-Mn**-(PhMeSO)], which may be considered a transition-state analogue for OAT from (oxo)manganese(V) corrole (no crystal structure of the Mn^V complex is available as yet) to sulfides, exhibits also a pyramidal structure with a domed conformation of the Mn−corrole entity. The sulfoxide ligand is strongly coordinated to the metal ion, as it is reflected by a relatively large deviation of Mn from the corrole plane (by 0.34 Å) and the short Mn−O$_{sulfoxide}$ bond (2.13 Å).

In all structures of corroles, as well as in the related porphyrin macrocycles (whether in the free-base or metalated form), the *meso*-substituted aryl groups are rotated with respect to the macrocyclic ring, in order to avoid severe steric hindrance between the aryls (and in particular the substituents in their *ortho* positions) and the adjacent pyrrole rings (and their C−H or C−R fragments in β positions). The dihedral angles between the mean planes of the aryl groups and of the central core usually vary

(20) (a) Harrison, H. R.; Hodder, O. J. R.; Hodgkin, D. C. *J. Chem. Soc. B* **1971**, 640–645. (b) Simkhovich, L.; Goldberg, I.; Gross, Z. *J. Inorg. Biochem.* **2000**, *80*, 235–238. (c) Paolesse, R.; Marini, A.; Nardis, S.; Frolio, A.; Smith, K. M. *J. Porphyrins Phthalocyanines* **2003**, *7*, 25–36. (d) Ding, T.; Harvey, J. D.; Ziegler, C. J. *J. Porphyrins Phthalocyanines* **2005**, *9*, 22–27. (e) Goldschmidt, R.; Goldberg, I.; Balazs, Y.; Gross, Z. *J. Porphyrins Phthalocyanines* **2006**, *10*, 76–86.

(21) Ou, Z.; Erben, C.; Autret, M.; Will, S.; Rosen, D.; Lex, J.; Vogel, E.; Kadish, K. M. *J. Porphyrins Phthalocyanines* **2005**, *9*, 398–412.

(22) Licoccia, S.; Morgante, E.; Paolesse, R.; Polizio, F.; Senge, M. O.; Tondello, E; Boschi, T. *Inorg. Chem.* **1997**, *36*, 1564–1570.
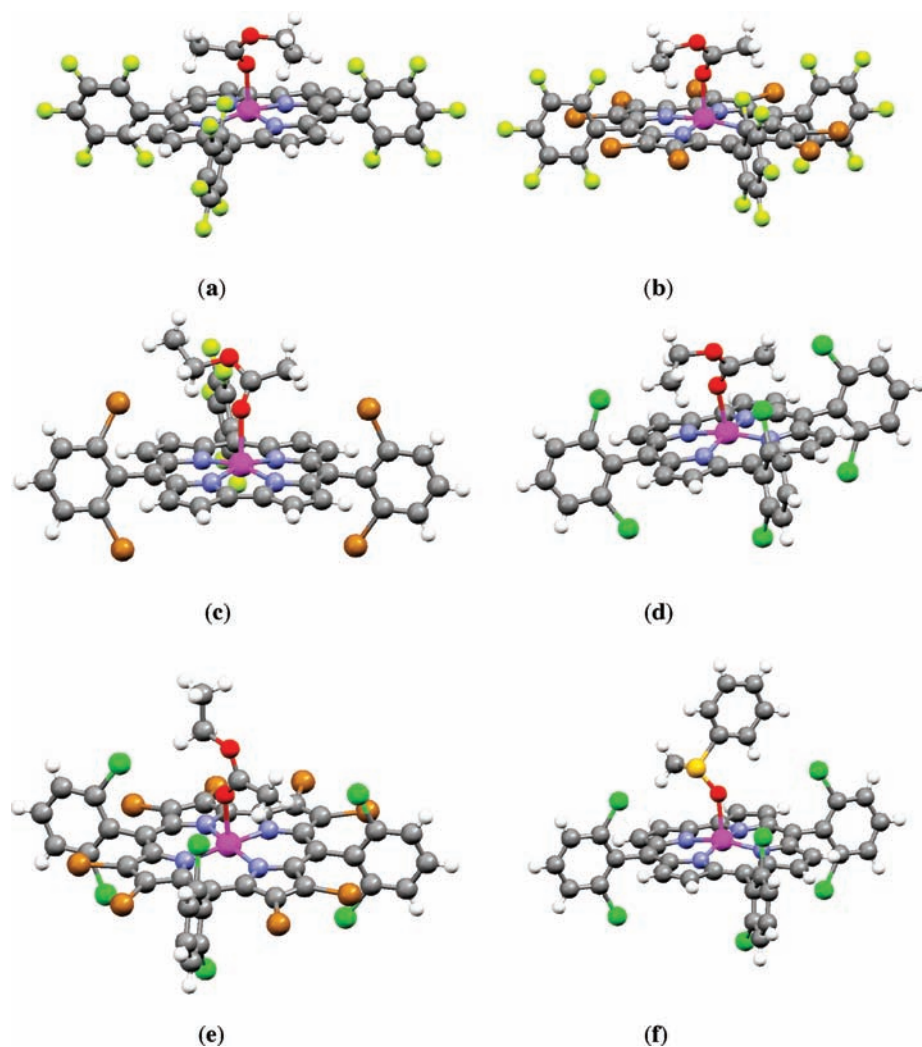
Figure 10. Molecular structures of (a) [**1-Mn**(OEtAc)], (b) [**1a-Mn**(OEtAc)], (c) [**3-Mn**(OEtAc)], (d) [**5-Mn**(OEtAc)], (e) [**5a-Mn**(OEtAc)], and (f) [**5-Mn**(PhMeSO)].

from about 60° to 90°. The specific values, observed in a given structure, are affected by the balance of secondary intramolecular (e.g., steric hindrance between the substituents on the aryl and pyrrole rings, attraction/repulsion of the *o*-aryl substituents to/ from the π-cloud of the corrole macrocycle or the axial ligand(s) if present) as well as intermolecular (e.g., π−π stacking or T-shaped arrangement between the aryls of adjacent molecules in the crystal) interactions. The corresponding dihedral angles observed in the manganese(III) complexes reported herein are listed in Table 1. The observed conformations in these structures seem to optimize in particular van der Waals contacts between the electronegative F, Cl, and Br substituents of the corrole and the C−H bonds of the axial ligands, which are apparently associated with the nearly perpendicular orientation of some of the Cl- and Br-substituted aryls to the corrole macrocycle (Figure 10). The axially bound ligands suffer no serious steric repulsions by the *o*-phenyl substituents, which may be appreciated from Figure 10c (EtOAc and 2,6-dibromophenyl) and Figure 10f (phenyl methyl sulfoxide and 2,6-dichlorophenyl). This conclusion is important for evaluating substrate approach to (oxo)manganese(V) corroles.

3.2.4. Electrochemistry. The electrochemistry of manganese(III) corroles was first described for derivatives with β-pyrrole alkyl-substituents such as octaethylcorrole (OEC),

followed by much later studies of *meso*-aryl-substituted corroles.[11e,23,24] The manganese(III) corroles are usually air stable (with one exception),[21] but can still be oxidized at relatively low potentials to manganese(IV) derivatives: 5-coordinated complexes with Cl⁻, Br⁻, and even I⁻ as a fifth axial ligand were isolated and fully characterized.[11e,24f] Since axial ligands from the electrolyte may significantly affect the redox potentials,[11b−d,21,24,26] the cyclic voltammograms of all complexes were recorded in the coordinating solvent acetonitrile. The presence of *meso*-substituents and the absence of β-pyrrole alkyls in the currently examined complexes enhance the first oxidation potential by 300−380 mV relative to the manganese(III) complex of OEC and similar corroles that are much more electron-rich.[25] The first oxidation potentials of the **1-Mn** to **5-Mn** series (Table 2) are, however, still lower by more than 300 mV relative to those of the manganese(III) tetraarylporphyrins, consistent with the known stabilizing effect of corroles regarding high-valent metal ions.[26] Bromination of the β-pyrrole carbon atom, i.e. transformation to the **1a-Mn** to **5a-Mn** complexes, leads to an increase in the first oxidation potential by 160−370 mV. Variations in the first oxidation potential of

(23) Shen, J.; Ojaimi, M. E.; Chkounda, M.; Gros, C. P.; Barbe, J.-M.; Shao, J.; Guillard, R.; Kadish, K. M. *Inorg. Chem.* **2008**, *47*, 7717–7727.

Table 2. Oxidation Potentials (vs Ag/AgCl) of the Various Manganese(III) Complexes and Reduction Potentials of the (Oxo)manganese(V) Corroles, in Acetonitrile with TBAP As Electrolyte[a]

complex	$E_{1/2}$ (V)	complex	$E_{1/2}$ (V)	Δ[b]	complex	$E_{1/2}$ (V)
1-Mn	0.62	**1a-Mn**	0.99	0.37	**1-Mn(O)**	0.17
2-Mn	0.65	**2a-Mn**	1.04	0.39	**2-Mn(O)**	0.10
3-Mn	0.68	**3a-Mn**	0.88	0.20	**3-Mn(O)**	0.06
4-Mn	0.68	**4a-Mn**	0.85	0.17	**4-Mn(O)**	0.10
5-Mn	0.64	**5a-Mn**	0.80	0.16	**5-Mn(O)**	0.01

[a] Fc/Fc$^+$ couple was measured as 0.44 V under identical conditions. [b] $E_{1/2}$ of brominated − $E_{1/2}$ of nonbrominated analogue.

1-Mn to **5-Mn** (i.e., as a function of substituents on the *meso*-aryls) are not significant, which is consistent with a metal-centered redox process. The relatively small shift in oxidation potential upon bromination (compared to a 530 mV for 6-coordinated iridium(III) corroles,[24g] as well as the significant variation of the effect of bromination within the current series (fifth column of Table 1), suggest that the effects of the *meso*-aryl groups is a combination of electronic (F > Cl, > Br > OMe) and steric (Br > Cl > F) effects of their substituents. We note that that 2,6-dihalophenyls have actually been demonstrated to sometimes act as electron-donating rather than electron-withdrawing substituents in tetraarylporphyrins.[27]

The reasonable thermal stability of the (oxo)manganese(V) corroles allowed for their examination by cyclic voltammetry as well (Figure 11 and Table 2), revealing redox processes that are clearly absent in their manganese(III) precursors. The slightly positive potentials are consistent with metal reduction ([Mn^V(O)]/Mn^{IV}(O)]$^-$), and the particular values suggest that **1-Mn(O)** ($E_{1/2}$ = 0.17 V) and **5-Mn(O)** ($E_{1/2}$ = 0.01 V) should be the strongest and the weakest oxidants, respectively. A comparison with published reduction potentials of (oxo)manganese(V) complexes chelated by other ligands reveals an $E_{1/2}$ of 0.02 V for the very stable (and nonreactive) corrolazine complex (in acetonitrile), 0.75 V for salen (computed value), and >1 V for tetrarylporphyrins (the macrocycle is oxidized prior to the metal). It is also interesting and important that the reduction potential of the (oxo)chromium(V) complex of corrole **1** (**1-Cr(O)**) is quite similar to that of **1-Mn(O)**.[11d,e,l] The relevance of large differences in reduction potentials of metal−oxo species to

(24) (a) Kadish, K. M.; Adamian, V. A.; Caemelbecke, E. V.; Gueletii, E.; Will, S.; Erben, C.; Vogel, E. *J. Am. Chem. Soc.* **1998**, *120*, 11986–11993. (b) Steene, E.; Wondimagegn, T. W.; Ghosh, A. *J. Phys. Chem. B* **2001**, *105*, 11406–11413. (c) Fryxelius, J.; Eilers, G.; Feyziyev, Y.; Magnuson, A.; Sun, L.; Lomoth, R. *J. Porphyrins Phthalocyanines* **2005**, *9*, 379–386. (d) Xia, M.; Liu, J.; Gao, Y.; Akermark, B.; Sun, L. *Helv. Chim. Acta* **2007**, *90*, 553–561. (e) Gao, Y.; Liu, J.; Wang, M.; Na, Y.; Åkermark, B.; Sun, L. *Tetrahedron* **2007**, *63*, 1987–1994. (f) Broring, M.; Hell, C.; Brandt, C. D. *Chem. Commun.* **2007**, 1861–1862. (g) Palmer, J. H.; Day, M. W.; Wilson, A. D.; Henling, L. M.; Gross, Z.; Gray, H. B. *J. Am. Chem. Soc.* **2008**, *130*, 7786–7787. (h) Liu, H. Y.; Chen., L.; Yam, F.; Zhan, H. Y.; Ying, X.; Wang, X. L.; Jiang, H. F.; Chang, C. K. *Chin. Chem. Lett.* **2008**, *19*, 1000–1003.

(25) Erben, C.; Will, S.; Kadish, K. M. In *The Porphyrin Handbook*; Kadish, K. M., Smith, K. M., Guilard, R., Eds.; Academic Press: Burlington, MA, 2000; Vol. 2, pp 233−300.

(26) (a) Gross, Z.; Gray, H. B. *Adv. Synth. Catal.* **2004**, *346*, 165. (b) Kadish, K. M.; Van Caemelbecke, E.; Royal, G. In *The Porphyrin Handbook*; Kadish, K. M., Smith, K. M., Guilard, R., Eds.; Academic Press: Burlington, MA, 2000; Vol. 8, pp 1−114. (c) Kadish, K. M. The Electrochemistry of Metalloporphyrins in Nonaqueous Media. In *Progress in Inorganic Chemistry*; Lippard, S. J., Ed.; John Wiley: New York, 1986; Vol. 34, pp 435−605.

(27) Koerner, R.; Wright, J. L.; Ding, X. D.; Nesset, M. J. M.; Aubrecht, K.; Watson, R. A.; Barber, R. A.; Mink, L. M.; Tipton, A. R.; Norvell, C. J.; Skidmore, K.; Simonis, U.; Walker, F. A. *Inorg. Chem.* **1998**, *37*, 733–745.
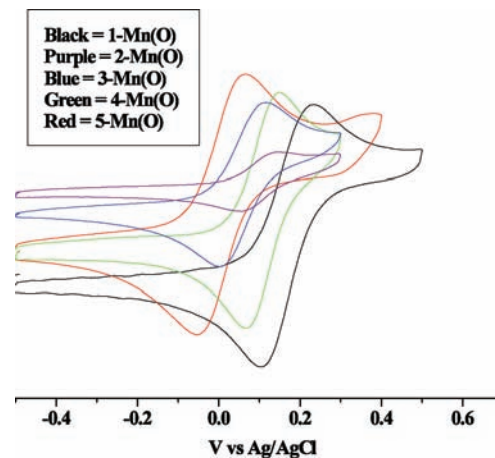
Figure 11. Cyclic voltammograms of **1-Mn(O)**−**5-Mn(O)**, in 0.5 M TBAP/acetonitrile solutions.

chemical reactivity, including OAT reactions, is relatively obvious. It is, however, important to keep in mind that a 1.0 V difference in reduction potentials between oxidant and reductant implies a 23 kcal/mol (the Faraday constant) thermodynamic barrier for a one-electron redox reaction. Nevertheless, despite the ~1.5 V reduction potential of thioanisole,[28] manganese(III) corroles are still good catalysts for its oxidation to the corresponding sulfoxides. Accordingly, and also in line with the earlier described mechanistic puzzles, it is of interest to examine if and how the different reduction potentials of the isolable (oxo)manganese(V) corroles come into effect in stoichiometric OAT reaction to sulfides.

3.3. Reactivity Studies. The first step in these investigations was to select the solvent in which (oxo)manganese(V) corroles are most stable, as to allow for kinetic studies of stoichiometric OAT reactions to organic substrates. Greenly colored solutions of the manganese(III) precursors **1-Mn** to **5-Mn** and **1a-Mn** to **5a-Mn** were treated with ozone in a dry ice/acetone bath, which induces a color change to red and brown for **1-Mn** to **5-Mn** and **1a-Mn** to **5a-Mn**, respectively. UV−vis spectroscopy examination of solutions that were warmed up to room temperature revealed that the apparent "survival times" of **1-Mn(O)**, **2-Mn(O)**, and **4-Mn(O)** were quite low in some solvents (THF, hexane, acetone, dichloromethane, and diethyl ether), but that they are stable for hours in ethyl acetate and acetonitrile. Accordingly, ethyl acetate was chosen for all investigations, despite the fact that **1a-Mn(O)** to **5a-Mn(O)** were most stable in dichloromethane and chloroform. The spontaneous decay rate constants (observed at 347 nm, 20 °C in ethyl acetate) for the transformations of (oxo)manganese(V) back to manganese(III) nm for 14.7 μM concentrations of **1-Mn(O)** to **5-Mn(O)** were in the range of 1.28×10^{-4} to 5.87×10^{-5} s^{-1}. Interestingly, the much more reactive **1a-Mn(O)** to **5a-Mn(O)** (*vide infra*) were thermally more stable than the less reactive **1-Mn(O)** to **5-Mn(O)**. This phenomenon may safely be attributed to the increased oxidation-resistance of brominated vs nonbrominated β-pyrrole double bonds in the corresponding corrole rings. More highly concentrated (oxo)manganese(V) corrole solutions decompose faster to their corresponding manganese(III) complexes, which may reflect disproportionation: the transformation of (oxo)manganese(V) corrole to (oxo)manganese(IV) and (oxo)manganese(VI) species. Sup-

(28) Trans-Goslinska, K.; Jonsson, M. *J. Phys. Chem. A* **2006**, *110*, 9513–9617.

Table 3. Rate Constants (M^{-1} s^{-1} $\times 10^3$) for Oxygen Transfer from the Nonbrominated (Oxo)manganese(V) Corroles (**1-Mn(O)** to **5-Mn(O)**) to *para*-Substituted Thioanisoles, in Ethyl Acetate at 20°C, As Measured by the Decay of the (Oxo)manganese(V) Characteristic Absorbance at 347 nm

X in 4-X—C_6H_4—S—CH_3	k, M^{-1} s^{-1} $\times 10^3$				
	1-Mn(O)	**2-Mn(O)**	**3-Mn(O)**	**4-Mn(O)**	**5-Mn(O)**
OCH_3	453	218.9	43.4	16.2	9.1
CH_3	179	135.4	29.6	17.2	8.8
H	116	106.4	16.3	15.5	7.9
Br	34	47.2	16.9	9.8	8.4
CN	6	18.1	5.6	7.9	5

porting evidence for this hypothesis is that **3-Mn(O)** and **5-Mn(O)** with their three 2,6-dichlorophenyl and 2,6-dibrorophenyl *meso*-substituents, respectively, were stable enough to be isolated as solids. This may be attributed to the combination of low reduction potential and steric protection against second order disproportionation.

Having confirmed reasonable stability of the (oxo)manganese(V) corroles, their reactivity with respect to oxygen transfer to various *para*-substituted thioanisoles at 20 °C was investigated. Upon addition of 1000 equiv of thioanisole to an ethyl acetate solution of **1-Mn(O)**, the initially red solution changed to green within a minute, thus signaling the transformation of **1-Mn(O)** to **1-Mn** by transferring its oxygen to the substrate. The corresponding spectral changes were characterized by a decrease in intensity at 347 nm and an increase at 482 and 600 nm. The linear dependence of the pseudo-first-order rate constant, obtained by following spectral changes at 347 nm, provided a second-order rate constant of 0.116 M^{-1} s^{-1}. Using identical procedures, the second-order rate constants were determined with various *para*-substituted thioanisoles (Table 3), as well as for the four other (oxo)manganese(V) corroles.

The rate constants for stoichiometric oxidation of ring-substituted thioanisoles by the five (oxo)manganese(V) corroles reveal that the order of reactivity for the three, more electron-rich sulfides is **1-Mn(O)** > **2-Mn(O)** ≫ **3-Mn(O)** > **4-Mn(O)** > **5-Mn(O)**. This pattern is in correlation with the number of C_6F_5-*meso*-substituents on their respective corrole skeleton: 3, 2, 1, 0, and 0, respectively. The pentafluorophenyl group may safely be predicted the most electron-withdrawing substituent among those present in the complexes, and its effect on destabilizing high-valent corrole and porphyrin complexes is both predictable and well supported by literature reports.[12-14,29] There may also be no doubt that the *p*-anisyl group is electron-donating, which is consistent with the reduced reactivity of **2-Mn(O)** (one anisyl and two C_6F_5 groups) relative to **1-Mn(O)** (three C_6F_5 groups). Reactivity further decreases from **3-Mn(O)** (one C_6F_5 and two 2,6-dibromophenyl groups) to **4-Mn(O)** and **5-Mn(O)**, which carry three 2,6-difluorophenyl and 2,6-dichlorophenyl groups, respectively. A more quantitative analysis of the effects of the aryls is not an obvious task because summing up Hammett σ constants of their substituents is not a reliable method, especially for *ortho*-substituents. On the other hand, established Hammett constants for all of the aryl groups exist only for pentafluorophenyl and *p*-anisyl ($\sigma = 0.27$ and -0.08, respectively),[30] but not for the 2,6-dihalophenyl groups that are
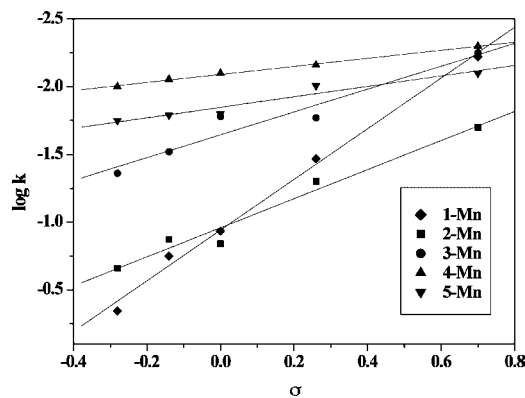

Figure 12. Hammett plots for the reactions of *para*-substituted thioanisoles with (oxo)manganese(V) corroles.

Table 4. Hammett ρ Values for the Reactions of **1-Mn(O)** to **5-Mn(O)** with *para*-Substituted Thioanisoles

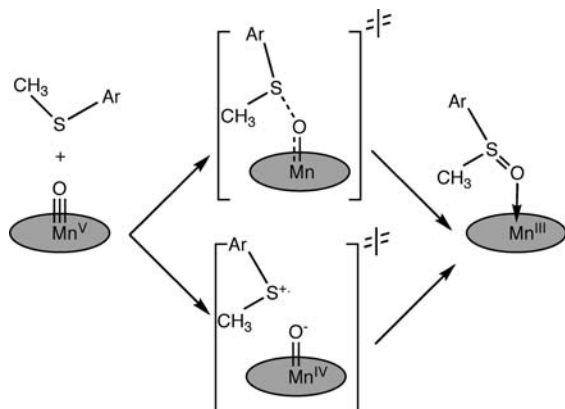| properties	**1-Mn(O)**	**2-Mn(O)**	**3-Mn(O)**	**4-Mn(O)**	**5-Mn(O)**
ρ (σ)	-1.87	-0.84	-1.06	-0.30	-0.39
correlation coefficient	0.9941	0.9693	0.9356	0.9954	0.9341

present in **5-Mn(O)**, **4-Mn(O)**, and **3-Mn(O)**. We further note that it has been shown that 2,6-dihalophenyls may actually behave as electron-donating substituents in tetraarylporphyrins.[27] Keeping these rather qualitative effects in mind, the results shown in Table 3 may be considered as consistent with expectations: the reactivity of the (oxo)manganese(V) complexes is a direct function of the electron-withdrawing capability of the aryls on the corrole. We further note that the correlation between the rate constants for OAT to sulfides by the (oxo)manganese(V) corroles and the reduction potentials of the latter (Table 2) is reasonable, but not perfect. Another issue is that the reactivity differences among the (oxo)manganese(V) corroles are much smaller for the less reactive sulfides: the rate constants for *p*-cyanothioanisole oxidation by the five (oxo)-manganese(V) corroles are almost identical.

The utilization of five *para*-substituted thioanisoles allows for construction of Hammett plots (Figure 12), which provide additional clues about some details of the reaction mechanism. Inspection of the corresponding ρ constants (Table 4) reveals negative values in all cases, consistent with the expected electrophilic character of the (oxo)manganese(V) corroles. The reactivity/selectivity principle is, however, clearly violated, as the most reactive complex **1-Mn(O)** is by far the most selective one ($\rho = -1.9$), followed by **2-Mn(O)** and **3-Mn(O)** ($\rho = -0.8$ and -1.1, respectively) and by extremely small selectivity for the least reactive **4-Mn(O)** and **5-Mn(O)** complexes ($\rho = -0.3$ and -0.4, respectively).

Within the framework of the single transition state drawn in Scheme 2 (top), a plausible explanation for the large ρ values in the most electron-poor and most oxidizing **1-Mn(O)** is that electron transfer from thioanisoles is relatively facile even without highly significant S—O bond formation. On the other hand, the importance of these nonsynchronous events may be reversed in the more electron-rich and hence less reducible complexes such as **4-Mn(O)** and **5-Mn(O)**. A somewhat different (but not necessarily conflicting) view is to (artificially) divide the overall process into two events: outer-sphere-like electron transfer, followed by S—O bond formation by the negatively charged (oxo)manganese(IV) corrole and the S-centered radical cation (Scheme 2, bottom). Since the ρ values
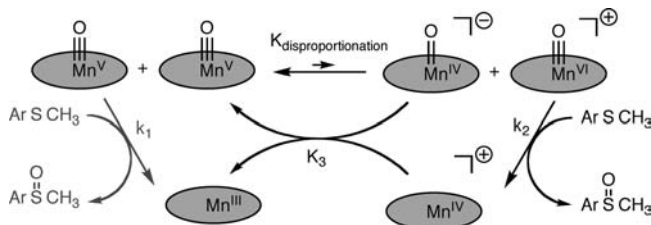
(29) (a) Pan, Z.; Newcomb, M. *Inorg. Chem.* **2007**, *46*, 6767–6774, and references therein. (b) Song, W. J.; Seo, M. S.; George, S. D.; Ohta, T.; Song, R.; Kang, M.-J.; Tosha, T.; Kitagawa, T.; Solomon, E. I.; Nam, W. *J. Am. Chem. Soc.* **2007**, *129*, 1268–1277.

(30) Hansch, C.; Leo, A.; Taft, R. W. *Chem. Rev.* **1991**, *91*, 165–196.

^{a} The contribution of pathway **b** (for any combination of a particular (oxo)manganese(V) complex and substrate) to the overall kinetics will increase as the transition-state energy for direct OAT increases (as illustrated by **a** and **c**).

for these two steps are expected to be opposite, the experimentally obtained value is indicative of their relative importance: becoming progressively less negative as the second step gains importance. The earlier discussed electrochemical data is relevant to this hypothesis as it clearly shows that single-electron transfer between these two partners is endogernic, most so for the least reactive **5-Mn(O)** and the least for the most reactive **1-Mn(O)**. In addition, it is well-known that the oxygen atom in triply bound metal−oxo complexes is of extremely low basicity and that the basicity increases very much in cases where one-electron reduction leads to a decreased bond order.[31] The (oxo)manganese(V) corroles fall into this category, since their initially low-spin d^2 state supports a triply bound metal−oxo bond, while the reduced complexes are high spin d^3 and hence only form a double bond with oxygen.[32] The most electron-rich (oxo)manganese(IV) corrole complexes may be safely predicted to be the most basic, which should lead to an increased importance of the S−O bond-formation step.

An alternative explanation is that the least facile reactions, i.e. those of **4-Mn(O)** and **5-Mn(O)** with all sulfides and of **1-Mn(O)** and **2-Mn(O)** with the electron-poor sulfides, proceed (partially or fully) via a very different mechanism because of the extremely poor driving force of the redox process. The earlier mentioned disproportionation hypothesis comes into account because the rate-limiting step in such cases might be the formation of (minutes amounts of) (oxo)manganese(VI) corrole, followed by fast and more thermodynamically favored OAT to the sulfides (Scheme 3). This could explain why the rate constants of **4-Mn(O)** and **5-Mn(O)** are relatively insensitive to the electron-richness of the sulfides (low ρ values) and why the least reactive sulfide reacts at very similar rates with all (oxo)manganese(V) corroles. This scenario is further illustrated in Scheme 4: pathway **a** is adopted for the combination of electron-poor (oxo)manganese(V) corroles and electron-rich sulfides, but as the transition-state energy of this direct OAT mechanism increases (illustrated by **c** in the Scheme), pathway **b** becomes progressively important. At the extreme situation (which apparently does not exist in the examples studied here), when only pathway **b** is adopted and disproportionation is fully rate-limiting, the rate constant would be identical for all substrates (i.e., reflected by a vanishing Hammett ρ value).
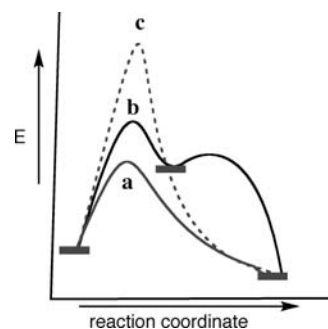
Independent evidence for the involvement of disproportionation was obtained by testing the reaction of a 147 μM solution of **4-Mn(O)** with thioanisole, in comparison with the standard condition of 14.7 μM. Despite the fact that the reactions were still pseudo-first-order (the sulfide concentrations were in the range of 15−75 mM), the second-order rate constant was about 2 times larger (0.014 vs 0.024 M^{-1} s^{-1}). This is a strong indication that the reaction is not purely first order in **4-Mn(O)**, hence strongly supporting the involvement of disproportionation and fast OAT from a highly reactive (oxo)manganese(VI) intermediate that displays little selectivity. Although the minute amounts of such intermediates preclude their detection by direct spectroscopic methods, we note that analogous (but more stabilized) (nitrido)manganese(VI) corroles have been characterized.[11j] Another important aspect is the reactivity of the (oxo)manganese(IV) corrole toward oxidation by nonoxo-stabilized manganese(IV) corrole (K$_3$ in Scheme 3), despite the reports regarding relatively easily isolated halide- and aryl-coordinated manganese(IV) corroles.[11e,33] The driving force in this case is the earlier mentioned increased bond order from 1 in (oxo)manganese(IV) to 3 in (oxo)manganese(V) corrole.

The oxygen transfer reaction of **2a-Mn(O)** to **5a-Mn(O)** with most thioanisoles is too fast to be measured by a stopped-flow spectrometer, and the second-order rate constants have hence been determined only for the relatively slow-reacting *p*-

(31) (a) Green, M. T.; Dawson, J. H.; Gray, H. B. *Science* **2004**, *304*, 1653–1656. (b) Green, M. T. *J. Am. Chem. Soc.* **2006**, *128*, 1902–1906.
(32) Visser, S. P. D.; Ogliaro, F.; Gross, Z.; Shaik, S. *Chem.—Eur. J.* **2001**, *7*, 4954–4960.

(33) (a) Broring, M.; Hell, C.; Brandt, C. D. *Chem. Commun.* **2007**, 1861–1862. (b) Broring, M.; Hell, C.; Steiner, M.; Brandt, C. D. *Z. Anorg. Allg. Chem.* **2007**, *633*, 1082–1086. (c) Broering, M.; Cordes, M.; Koehler, S. *Z. Anorg. Allg. Chem.* **2008**, *634*, 125–130.

Table 5. Kinetic Data for the Oxygen Transfer Reactions from Nonbrominated (in ethyl acetate) and Brominated (in dichloromethane) (Oxo)manganese(V) Corroles to *p*-Bromothioanisole at 20 °C

complex	rate constant (M^{-1} s^{-1})	complex	rate constant (M^{-1} s^{-1})
1-Mn(O)	0.034	**1a-Mn(O)**	3242
2-Mn(O)	0.047	**2a-Mn(O)**	3082
3-Mn(O)	0.017	**3a-Mn(O)**	1725
4-Mn(O)	0.0098	**4a-Mn(O)**	1464
5-Mn(O)	0.0084	**5a-Mn(O)**	896

bromothioanisole (Table 5). The reactivity order is **1a-Mn(O) > 2a-Mn(O) > 3a-Mn(O) > 4a-Mn(O) > 5a-Mn(O)** which is similar to that in the **1-Mn(O)** to **5-Mn(O)** series. The ~5 orders of magnitude differences in rate constants are quite nicely correlated with the differences in electrochemistry of the corresponding manganese(III) complexes (Table 2): the ~0.25 V more positive redox potentials of the brominated derivatives may be translated into a 6 kcal/mol decreased activation energy for electron transfer, which could in principle induce an up to 10 orders of magnitude in reactivity.

4. Summary and Conclusions

We have synthesized five triarylcorroles that differ significantly in steric crowding and in electron-withdrawing capability. The corresponding manganese(III) corroles were prepared; and these were converted into another series of manganese(III) complexes via bromination of the β-pyrrole CH bonds. The molecular structures of two new free-base corroles were obtained and found to be nonplanar so as to accommodate the three NH protons inside the corrole core. Six new manganese(III) complexes, including brominated and nonbrominated corroles, have been structurally characterized as well. In all cases, the manganese(III) ion is 5-coordinated (pentagonal pyramid) with the oxygen atom of ethyl acetate as axial ligand. We have also structurally characterized a transition-state analogue for the oxygen transfer from (oxo)manganese(V) corroles to thioanisole: a manganese(III) corrole that is coordinated by the oxygen atom of the corresponding sulfoxide. Cyclic voltammetry revealed that the brominated manganese(III) complexes are harder to oxidize than their corresponding nonbrominated derivatives by about 0.25 V. Treatment of both the brominated and the nonbrominated manganese(III) corroles with ozone leads to clean conversion into the corresponding (oxo)manganese(V) complexes. These diamagnetic d^2 low-spin species were fully characterized by ^{1}H and ^{19}F NMR spectroscopy, thus confirming the manganese–oxygen triple bond. The steric crowding provided by the *meso*-substituents plays an important role in stabilizing the (oxo)manganese(V) corroles, e.g. **5-Mn(O)** and

3-Mn(O) are stable for days in acetonitrile at room temperature. The thermal stability of the β-pyrrole-brominated (oxo)manganese(V) complexes is even larger than that of the nonbrominated derivatives, which may be attributed to the oxidation resistance of C–Br bonds relative to C–H bonds.

The reactivity studies focused on the main puzzle in oxidation reactions catalyzed by manganese(III) corroles, for which four OAT reaction intermediates have been proposed (Scheme 1). The utilization of ozone for the preparation of the (oxo)manganese(V) corroles and the investigation of their *stoichiometric* OAT reactions allowed for the attention on species **C** and **E**, since the oxidant-coordinated manganese(III) (**B**) and (oxo)manganese(V) corroles (**D**), may safely be ruled out under these conditions. The reactivity, in terms of OAT to sulfides, of the β-pyrrole-brominated (oxo)manganese(V) complexes is by 5 orders of magnitude larger than that of the nonbrominated derivatives. This observation, as well as the large negative Hammett ρ values obtained for OAT from **1-Mn(O)** to **3-Mn(O)** to a series of *para*-substituted thioanisoles, shows that (oxo)manganese(V) corroles are legitimate OAT agents. This conclusion is valid for the more reactive complexes, **1-Mn(O)** to **3-Mn(O)** and all the derivatives with β-pyrrole-brominated corroles, for which the driving force for the reaction is reasonable. The kinetic data of the least reactive derivatives **4-Mn(O)** and **5-Mn(O),** in particular the much less negative Hammett ρ values and the non-first-order dependence on their concentration, point toward a significant contribution of an alternative pathway in these cases. Disproportionation of (oxo)manganese(V) to [(oxo)manganese(VI)]$^+$ corrole and subsequent OAT to substrate by the latter is consistent with the data. The importance of these findings is that it is not limited to the studied case and hence much more far-reaching. We trust that they may also be of significant relevance to oxidation catalysis by other metal complexes, including manganese, iron, and ruthenium porphyrins and salens.[34]

Supporting Information Available: ^{1}H and ^{19}F NMR spectra and MS and cyclic voltammetry; reported X-ray structural data in CIF format. This material is available free of charge via the Internet at http://pubs.acs.org.

JA1050296

(34) (a) Fukuzumi, S.; Fujioka, N.; Kotani, H.; Ohkubo, K.; Lee, Y. M.; Nam, W. *J. Am. Chem. Soc.* **2009**, *131*, 17127–17134. (b) Pan, Z. Z.; Newcomb, M. *Inorg. Chem.* **2007**, *46*, 6767–6774. (c) Vanover, E.; Huang, Y.; Xu, L. B.; Newcomb, M.; Zhang, R. *Org. Lett.* **2010**, *12*, 2246–2249. (d) Zhang, R.; Horner, J. H.; Newcomb, M. *J. Am. Chem. Soc.* **2005**, *127*, 6573–6582. (e) Shimizu, H.; Onitsuka, S.; Egami, H.; Katsuki, T. *J. Am. Chem. Soc.* **2005**, *127*, 5396–5413.